MINISTÈRE DE LA TRANSITION ÉNERGÉTIQUE
Liberté Égalité Fraternité

TECNOAMBIENTE
A TRADEBE COMPANY

Document reference				***Issue information***	
Project	**Package**	**Issuer**	**Chrono**	**Revision**	**Status**
OLE_AO7	*-*	*TEC*	*00032*	*3*	*A*
Title	***OLE-TEC-00032_A_rev03_Factual report_Seismic survey – OWF area***				

Additional Metadata	**Discipline**	**Document Type**	**System**	**Activity**
	GPY	*Factual report*	*-*	*Seismic survey*
	Contract	**Acceptance Class**	**Dossier**	**Alternative ref.**
	AO6-AO7	*-*	*-*	*-*
	Confidentiality	**Print format**	**Subcontractor**	**Contractor ref.**
	Restricted	*A4*	*-*	*-*

Date	Rev	Status	Reason for revision	Issued by	Checked by	Approved by
19/09/2023	*0*	*IFR*	*Issued*	*BMC*	*MH*	*FLO*
02/11/2023	*1*	*B*	*Revision after client's comments*	*BMC*	*MH*	*FLO*
0712/2023	*2*	*B*	*Revision after client's comments*	*BMC*	*MH*	*FLO*
22/12/2023	*3*	*B*	*Revision after client's comments*	*BMC*	*MH*	*FLO*
12/01/2024	*3_A*	*A*	*Approved document*	*BMC*	*MH*	*FLO*

Change Log

Document uncontrolled when printed/downloaded.

Always check with document control for the latest revision.

TECNOAMBIENTE
A TRADEBE COMPANY

MINISTÈRE
DE LA TRANSITION
ÉNERGÉTIQUE
Liberté
Égalité
Fraternité

OLE_AO7 AREA – OWF
UHR SEISMIC SURVEY

OLE-TEC-00032_A_REV03_FACTUAL REPORT_SEISMIC SURVEY – OWF AREA

PROJECT No.
113401341

FACTUAL REPORT

No. OF PAGES
88

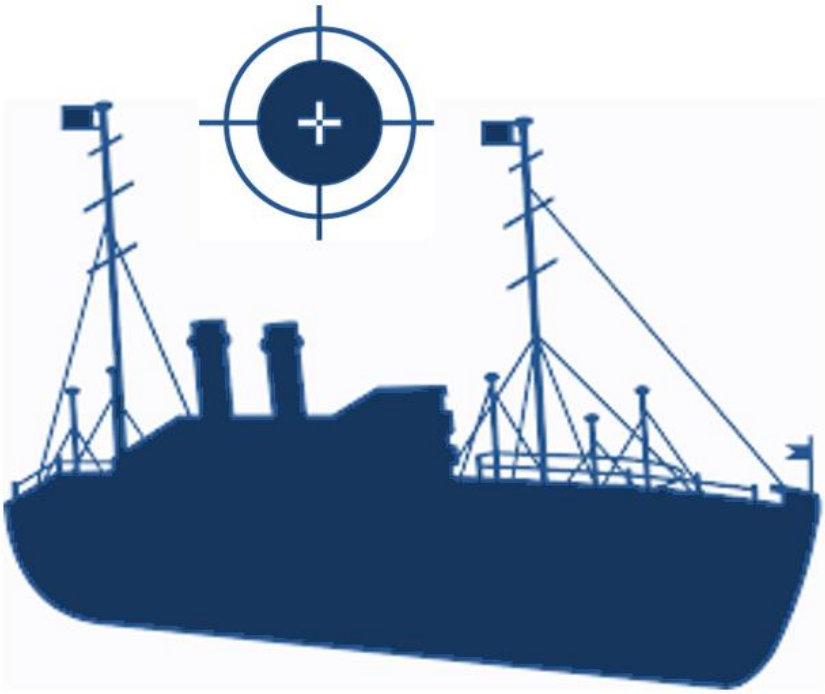

3_A	*12/01/2024*	*Approved document*	*BMC*	*MH*	*JW*	*FLO*	*DGEC*
3	*22/12/2023*	*Revision after client's comments*	*BMC*	*MH*	*JW*	*FLO*	*DGEC*
2	*07/12/2023*	*Revision after client's comments*	*BMC*	*MH*	*JW*	*FLO*	*DGEC*
1	*02/11/2023*	*Revision after client's comments*	*BMC*	*MH*	*JW*	*FLO*	*DGEC*
0	*19/09/2023*	*Issued*	*BMC*	*MH*	*JW*	*FLO*	*DGEC*
REV	***DATE***	***DESCRIPTION***	***BY***	***CHK***	***ENG***	***PM***	***CLIENT***

CONTENTS

EXECUTIVE SUMMARY 6
1. INTRODUCTION 6
1.1. PROJECT OVERVIEW 6
1.2. SCOPE OF WORK 10
1.3. GEODETIC PARAMETERS 10
1.3.1. Survey datum 10
1.3.2. Vertical datum 11
1.3.3. Tidal reduction 12
2. METHODOLOGY 13
2.1. MBES BATHYMETRY 13
2.1.1. Data acquisition 13
2.1.2. Data processing 15
2.2. UHR SEISMIC 16
2.2.1. Data acquisition 16
2.2.2. Data processing 19
3. RESULTS 23
3.1. BATHYMETRY 23
3.2. GEOLOGY 24
3.2.1. Geological setting from background data 24
3.2.2. Geological sequence 25
3.2.3. Geohazards 39
3.2.4. Conclusions and recommendations/comments 46
4. REFERENCES 48

APPENDIX I – CHARTING.....49

APPENDIX II – PROCESSING AND INTERPRETATION REPORT.....50

LIST OF FIGURES

Figure 1-1: OLE_AO7 survey area. 7

Figure 1-2: Windfarm areas (OWF) and Offshore Substations (OSS) in the OLE_AO7 survey area.....8

Figure 1-3: Line plan for OLE_AO7 Zone 1 Windfarm area (OWF).....9

Figure 1-4: QINSy's method for accurate tide calculation. 12

Figure 2-1: MBES bathymetry data acquisition with the QINSy software. 14

Figure 2-2: Processing screen of MBES bathymetry data with the Qimera software.....15

Figure 2-3: 3D image of the MBES bathymetry processing. 15

Figure 2-4: MBES bathymetry processing overview. 16

Figure 2-5: Screenshot from Geometrics LH16 software during UHR Seismic acquisition. 18

Figure 2-6: UHR Seismic processing overview.....20

Figure 2-7: Minimum phase brute stack.....21

Figure 2-8: Zero-phase corrected control stack (Demultiple, Noise filtering, Deghost, Static Correction, Far Trace Mute & Pre-Stack Migration).....22

Figure 2-9: Zero-phase corrected final processed stack (Time-Variant Bandpass filter, FK filter, Gain balancing) 22

Figure 3-1: Bathymetric data grid model (1 x 1 m) for the OLE_AO7 OWF Parcs 1 and 2 24

Figure 3-2: Line OLE_OWF_ M07. 30

Figure 3-3: Line OLE_OWF_ X07.....31

Figure 3-4: Data example through BH04. 32

Figure 3-5: Ribbon plot of Unit 1 (H05).....34

Figure 3-6: Isochore of H10, depth below seabed (base Unit 2). 35

Figure 3-7: Isochore of H20, depth below seabed (base Unit 3). 36

Figure 3-8: Isochore of H30, depth below seabed (base Unit 4). 37

Figure 3-9: Thickness of Quaternary Sequence. 38
Figure 3-10: Gas hazards. 41
Figure 3-11: Illustrating the Main Faults within the bedrock. 42
Figure 3-12: Example of gas anomalies (Gas Level 1). 43
Figure 3-13: Example of gas anomalies (Gas Level 2). 44

LIST OF TABLES

Table 1: Datum parameters table 10
Table 2: Projection parameters table. 11
Table 3: UHRS operational parameters. 17
Table 4: Available borehole data from BH04. 25
Table 5: Shallow geological units. 33
Table 6: Geological characteristics / processes and potential constraints. 45

ABBREVIATIONS

ADCP	Acoustic Doppler Current Profiler
ASV	Assumed Sound Velocity
Ch	Channel
cm	Centimetre
CMP	Common Mid-Point
C-O	Computed Minus Observed
CoG	Centre of Gravity
CRP	Central Reference Point
CSP	Central Shot Point
DEMOB	Demobilisation
DGEC	Direction générale de l'énergie et du climat
DP	Dynamic Positioning
DPO	Dynamic Positioning Officer
DPR	Daily production report
EP	Environmental Protection
FLO	Fisheries Liaison Officer
GNSS	Global Navigation Satellite System

ABBREVIATIONS

GPS	Global Positioning System
GRS	Geodetic Reference System
GSO	Geophysical Services Offshore
h	Hour
IMO	International Maritime Organization
J	Joule
JNCC	Joint Nature Conservation Committee
kHz	Kilohertz
LAT	Low Astronomical Tide
m	Meters
min	Minutes
MBES	Multibeam echosounder
MDAC	Marine Derived Authigenic Carbonates
mm	Millimetre
MOB	Mobilisation
MRU	Motion Reference Unit
POB	Personnel On Board
PAM	Passive Acoustic Monitoring
PPP	Precise Point Positioning
PPSU	Pulse Power Supply Unit
QA-QC	Quality Assurance – Quality Control
RTE	Réseau de Transport d'Électricité
RTK	Real Time Kinematics
s	Second
SHOM	Service Hydrographique et Océanographique de la Marine
SN	Serial Number
SRF	Ship's Reference Frame
SVP	Sound Velocity Profiler
SVS	Sound Velocity Sensor
TBC	To be confirmed
TTS	TTSurvey Ltd (Seismic equipment hire company)
UHR	Ultra-High Resolution

ABBREVIATIONS

UTC	Coordinated Universal Time
UTM	Universal Transverse Mercator
VSAT	Very-Small-Aperture Terminal
WB	Water Bottom
WD	Water Depth
WGS84	World Geodetic System 1984
WT	Work time
ZH	Hydrographic Zero or Hydrographic Datum

EXECUTIVE SUMMARY

According to the detected bathymetric results in the acquired lines of the offshore windfarm survey area, the water depths range between -52.96 meters (ZH) in the shallowest part at the south-eastern region, to -83.45 meters (ZH) in the north-western region.

The seabed slopes are gentle, with average seabed gradients of 0.71°, maximum values of 81.18º and minimum values of 0º.

The Bay of Biscay formed during the opening of the North Atlantic during the Late Cretaceous, with the rotation of the Iberian Peninsula. A thin succession of Late Pleistocene silty sand and clay are predicted across much of the area with much older Calcarenite also within the upper 30m sub-seabed. Calcarenite outcrops in the east of the survey area.

Two levels of shallow gas are present within the windfarm area.

1. INTRODUCTION

1.1. PROJECT OVERVIEW

The area of interest, corresponding to the windfarm and OSS sites, is in the Gulf of Gascogne, 40km off the coast of the Ile d'Oléron. The area of interest is approximately 24km x 20km and according to the SHOM bathymetry, the site is located in water depths ranging from --52 to -83m (Figure 1-1).

The offshore windfarm area is divided in two sites:

- Parc 1 (East), with an approximate area of 150 km^2.
- Parc 2, (West) with an approximate area of 280 km^2.

The total area of the windfarm is 430 km^2, which has been surveyed as a single area. As for the offshore substations, two separate ones have been determined, located at each of the offshore windfarms (Figure 1-2):

- Parc 1. One OSS area at the eastern edge of the wind farm, 4 km^2.
- Parc 2. Two OSS area options of 2km² are considered, OSS-2W and OSS-2E, located respectively in the north-west corner and the northern edge of the site.

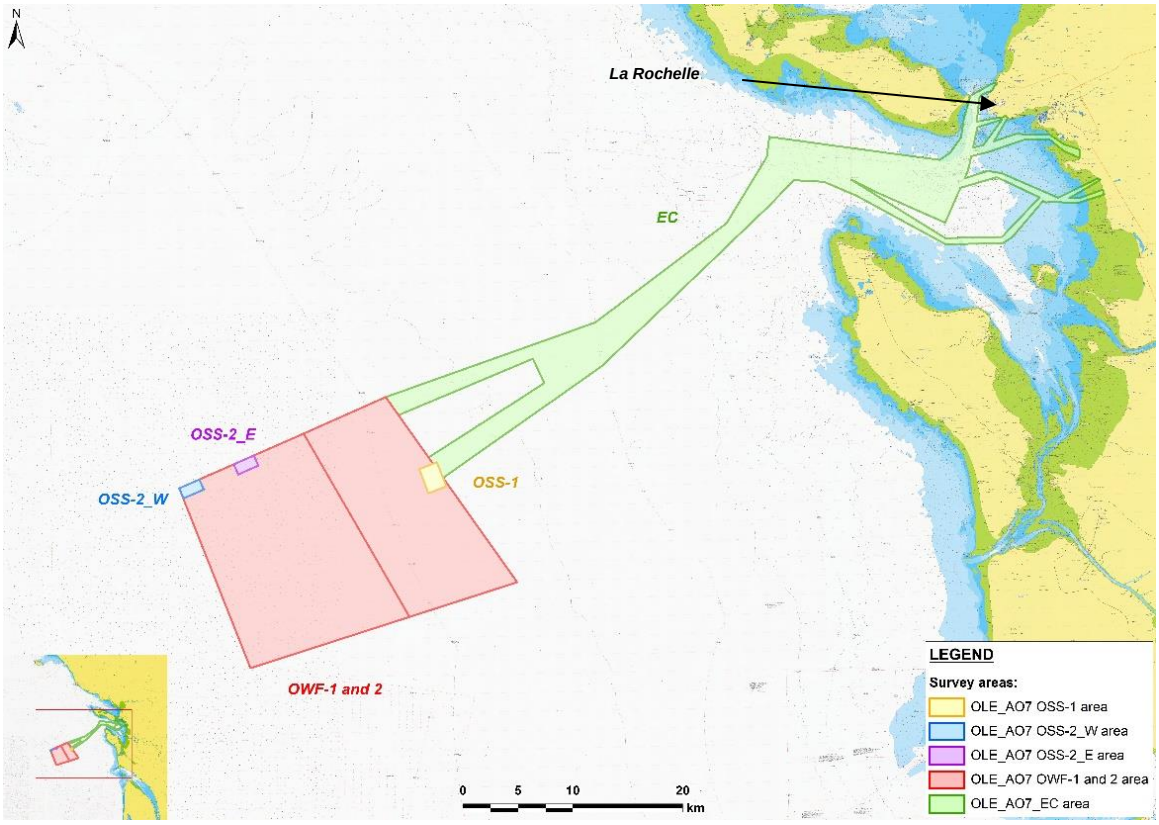

Figure 1-1: OLE_AO7 survey area.

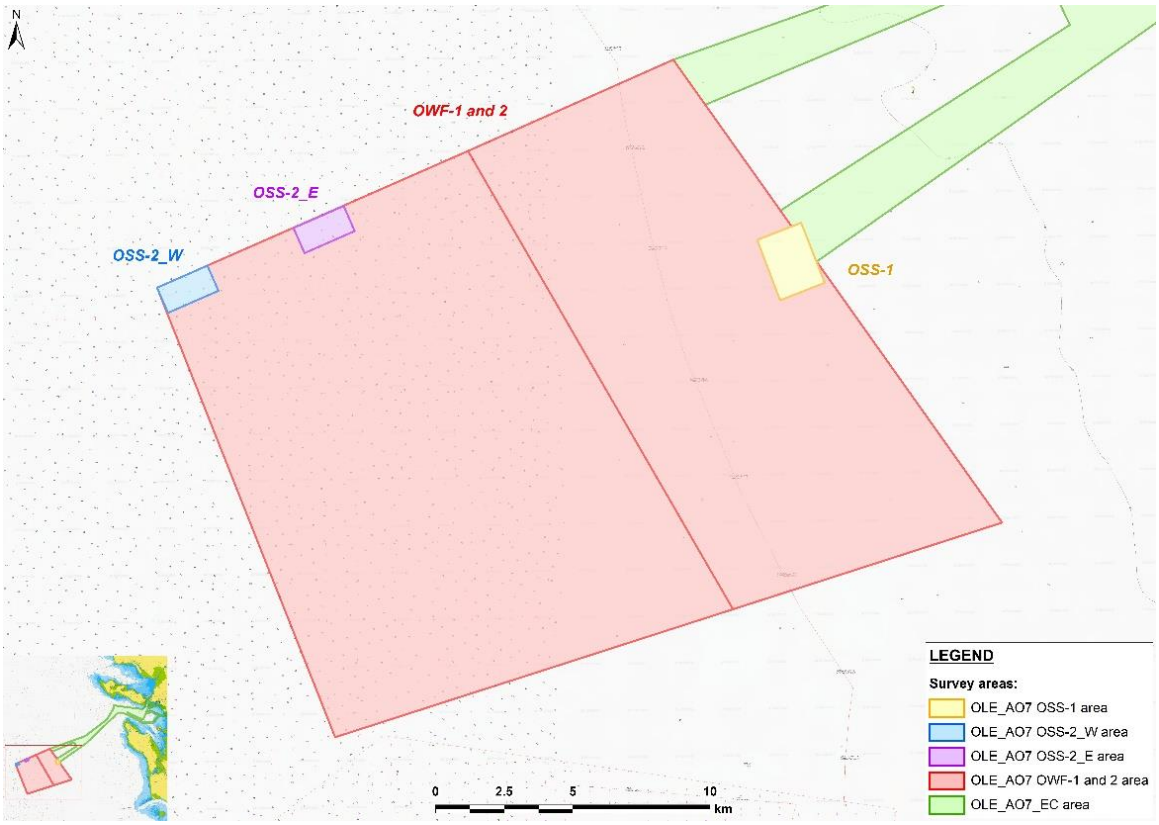

Figure 1-2: Windfarm areas (OWF) and Offshore Substations (OSS) in the OLE_AO7 survey area.

Figure 1-3 shows the survey line plan for MBES, SBP and UHRS data acquisition for all acquired survey lines over the OWF area.

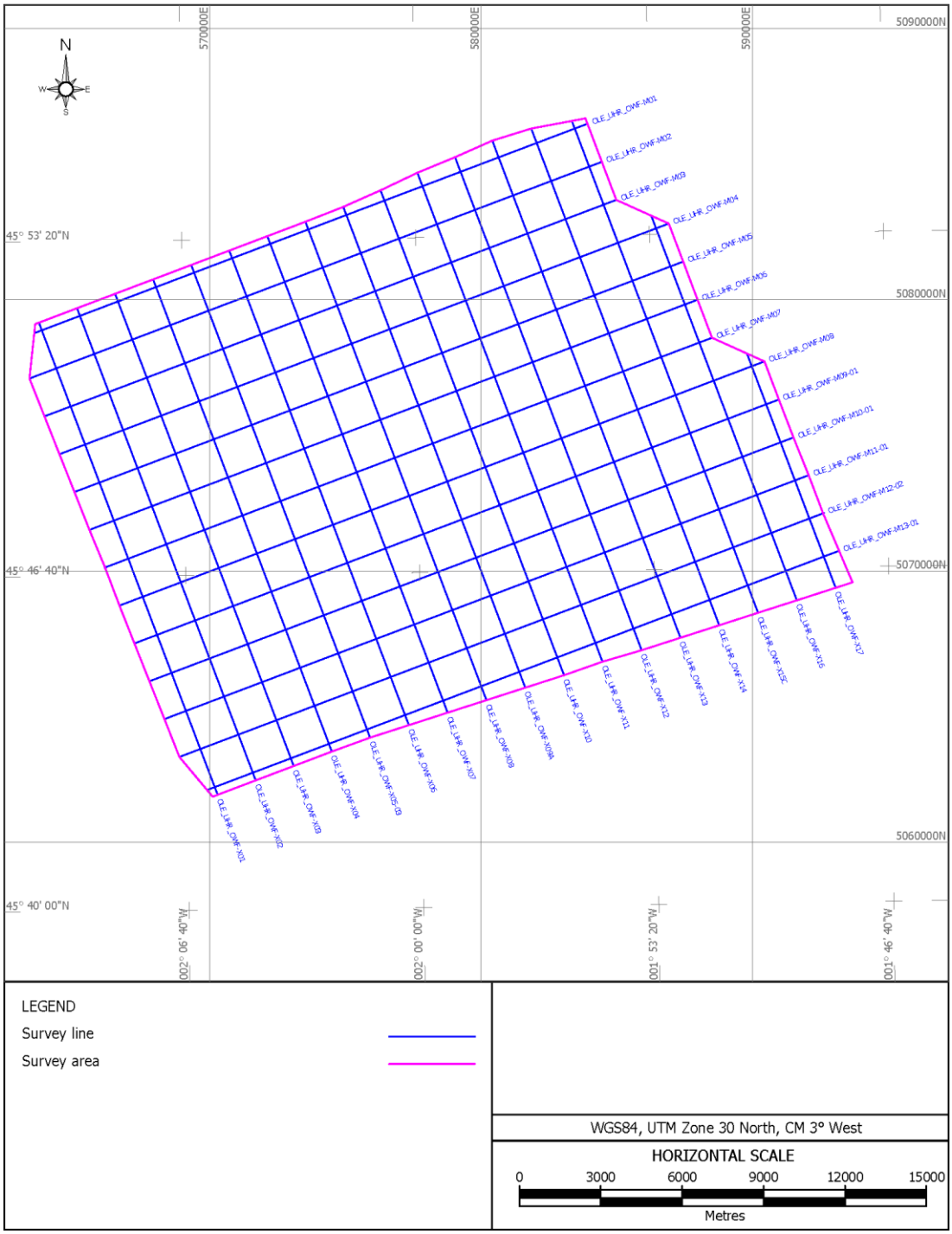

Figure 1-3: Line plan for OLE_AO7 Zone 1 Windfarm area (OWF).

1.2. SCOPE OF WORK

The objective of the site survey was to perform a geophysical survey over the proposed OWF and OSS sites comprising MBES, and UHRS datasets. The purpose of this was to:

- To define the water depths and seabed topography.
- To define the shallow (nominally 30 m BSB) subsurface geology.
- Identify any potential geohazards

The main purpose of the study is to provide an interpretation of the geophysical data to better understand the main characteristics of the seabed and geology at the project location and to undertake a derisking study over the OLE_AO7 Zone OWF site.

1.3. GEODETIC PARAMETERS

1.3.1. Survey datum

These parameters are detailed below.

Table 1: Datum parameters table

DATUM	
Survey Datum:	WGS 84
Spheroid	GRS 1980
Semi-Major Axis (a)	6378137.000000000
Semi-Minor Axis (b)	6356752.314245179
Inverse Flattening (1/f)	1/298.257223563

Table 2: Projection parameters table.

PROJECTION	
Projection	UTM
False Easting	500000
False Northing	0
Latitude of Origin	0º00’00.000000’’
Central Meridian	3º00’00.000000’’
UTM Zone	30 N
Scale Factor on CM	0.9996
Units:	Meters

1.3.2. Vertical datum

The vertical datum used in the QINSy software is Bathyelli v2.0 ZH geoid published by the SHOM in 2018. The Bathyelli v2.0 ZH (2018) is a surface based on the GRS 1980 spheroid, and it is a set of surfaces each of which defines the separation of one vertical datum from the WGS84 ellipsoid to the vertical maritime reference Hydrographic Datum or Hydrographic Zero. These ellipsoidal heights are given in metres.

This geoid covers the intersection between the SHOM tidal model and the different tidal zones of France.

For the OLE_AO7 survey area, the corrections to hydrographic zero are made by tidal observations at the port Port-La Rochelle-La Pallice (46º 10’ N, 01º 13’ W). For informative purposes, the difference between the hydrographic zero and the LAT reference level for this port is 0.17 m, according to the study by SHOM "*Références Altimétriques Maritimes. Ports de France métropolitaine et d'outre-mer"* of 2019.

1.3.3. Tidal reduction

Tecnoambiente received MarineStar PPP corrections by satellite. When using an accurate GNSS system, tidal corrections were carried out in real-time through QINSy computations, as shown in the next figure.

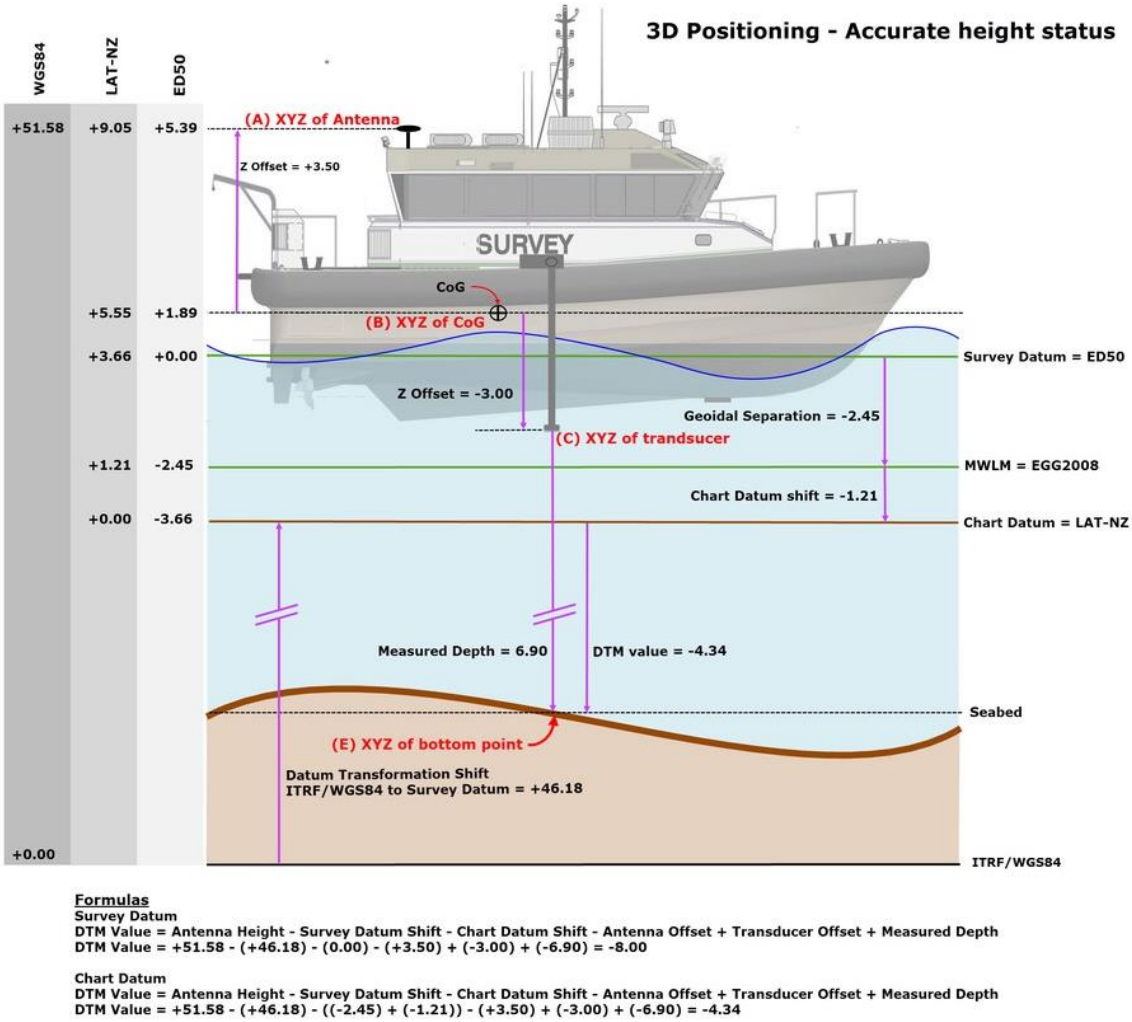

Figure 1-4: QINSy's method for accurate tide calculation.

Dropped corrections were applied in post processing.

2. METHODOLOGY

2.1. MBES BATHYMETRY

2.1.1. Data acquisition

The MBES data has been acquired only along the seismic lines, with an objective of calibrating the seismic data in depth. Therefore, the MBES data has been acquired along trackline with a spacing of 1500 meters.

During the data acquisition, the vessel's master must follow the previously programmed routes of the project lines, governed by the indications of the computer screen (Helmsmann indicator), which is shown, by means of visual and audible alarms, when it separates from its course more than a specified amount (variable according to weather conditions in the area, but never more than 2.5 metres from the theoretical line), and also when there is a problem in a peripheral, such as the loss of GPS corrections.

While the master follows the navigation lines, the acquisition module of the hydrography program captures all the position data sent by the GPS, as well as the soundings sent by the multibeam sounder for each transmission pulse, as well as the values of the heading, wave height, roll and head angles sent by the MRU.

Parallel to the data entry, the data acquired by the equipment and peripherals is synchronized. This process is carried out using the hydrographic processing software QINSy, complemented by the input of the time and the pulse per second (PPS) provided by the MRU, so that all the data is time synchronised.

The guidelines followed by Tecnoambiente during the survey for MBES data acquisition were the following ones:

- IT-CM-01 Guidelines for Hydrography Project management, 5;
- IT-CM-04. Bathymetric survey, 1
- IT-CM-14 Survey Basics Guidance, 1
- IT-CM-15 Online Surveying procedure, 3

These guidelines can be found in the quality plan document OLE_TEC_00004_IFE_rev02 - Quality Plan.

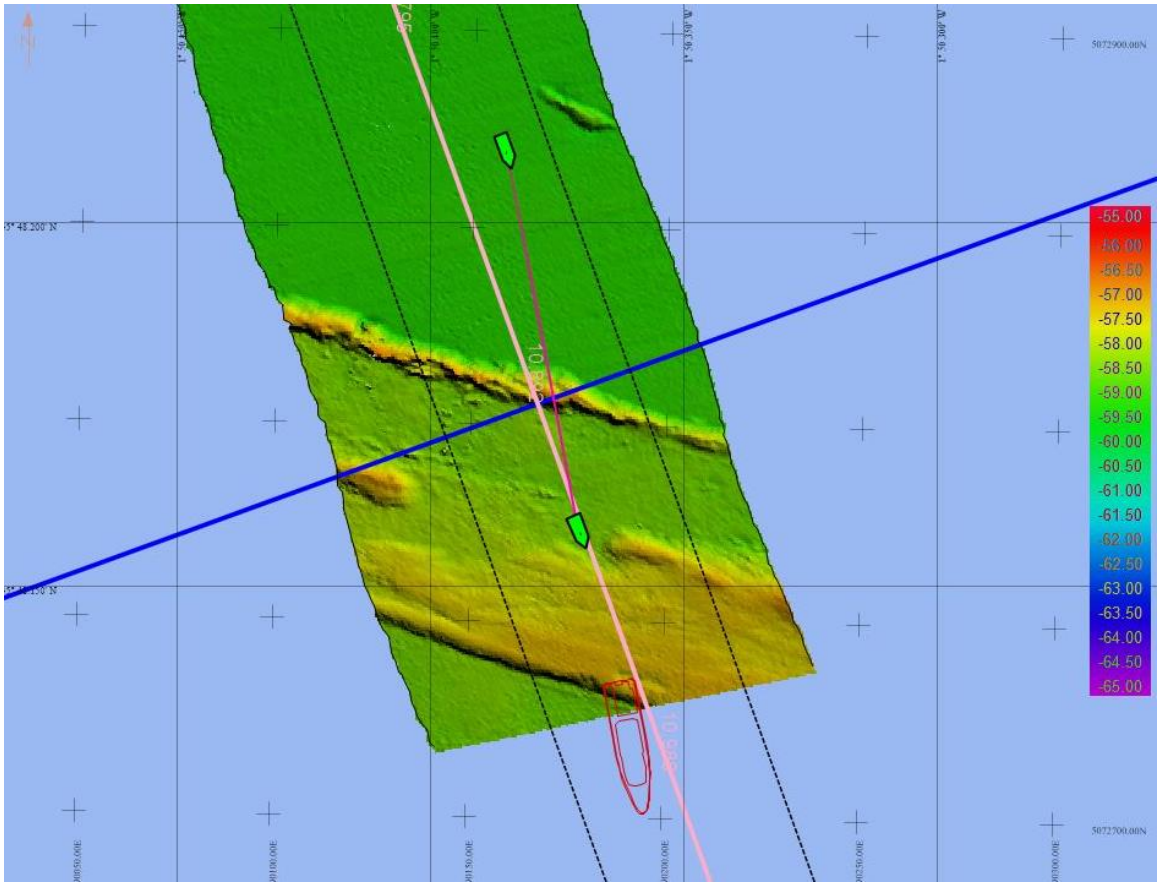

Figure 2-1: MBES bathymetry data acquisition with the QINSy software.

The heave of the MBES data was corrected online while acquiring the data, when aligning the seismic data in the profile this correction is applied. In order to do so, the MBES DTM model was time-shifted into the UHRS project.

2.1.2. Data processing

Along the processing phase of the acquired data, the lines on the screen are processed in order to manually match the height of the bathymetric lines and also correct the noise that appears in the records, noise produced by multiple factors such as, multipath in position, air bubbles, motor interference of the vessel etc. in the digital register of soundings.

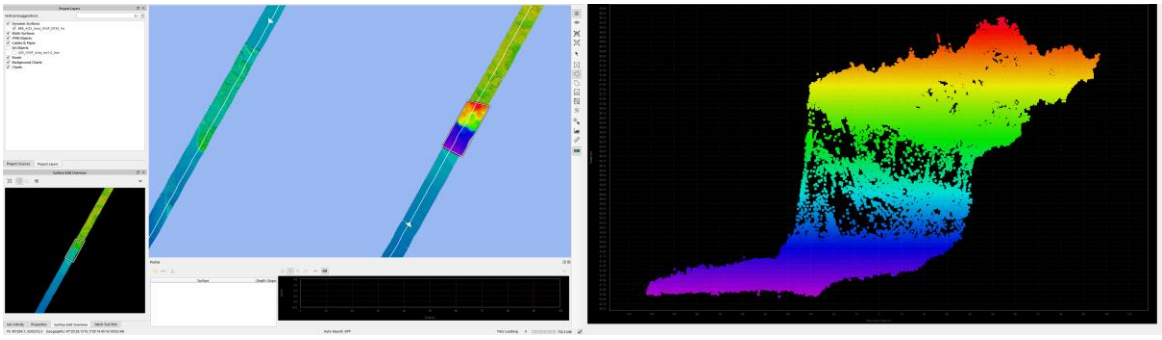

Figure 2-2: Processing screen of MBES bathymetry data with the Qimera software.

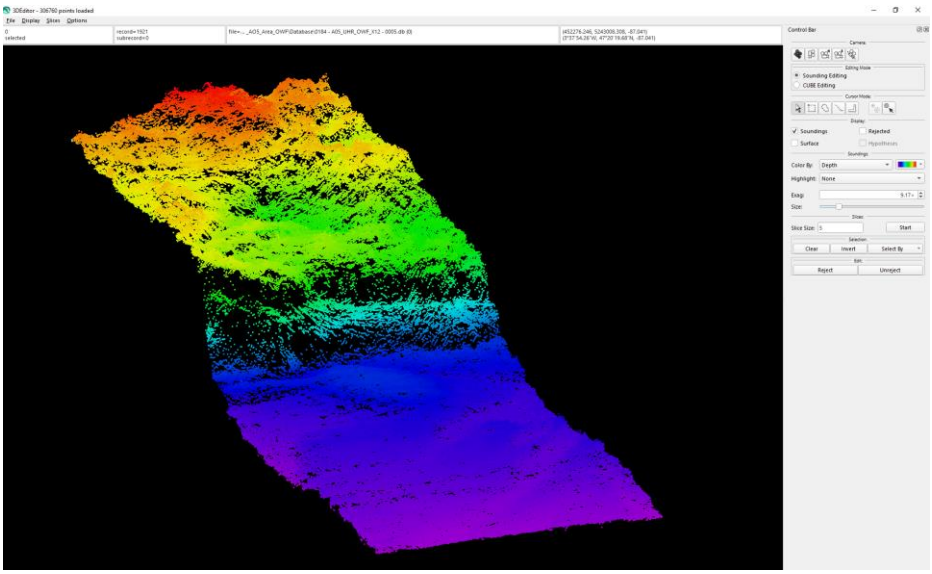

Figure 2-3: 3D image of the MBES bathymetry processing.

Once the possible existing errors in the records have been deleted, a digital model of the terrain with 1 x 1 m grid size has been made with a minimum cell size to obtain the maximum resolution of the seabed.

The general MBES processing workflow is presented in the following figure.

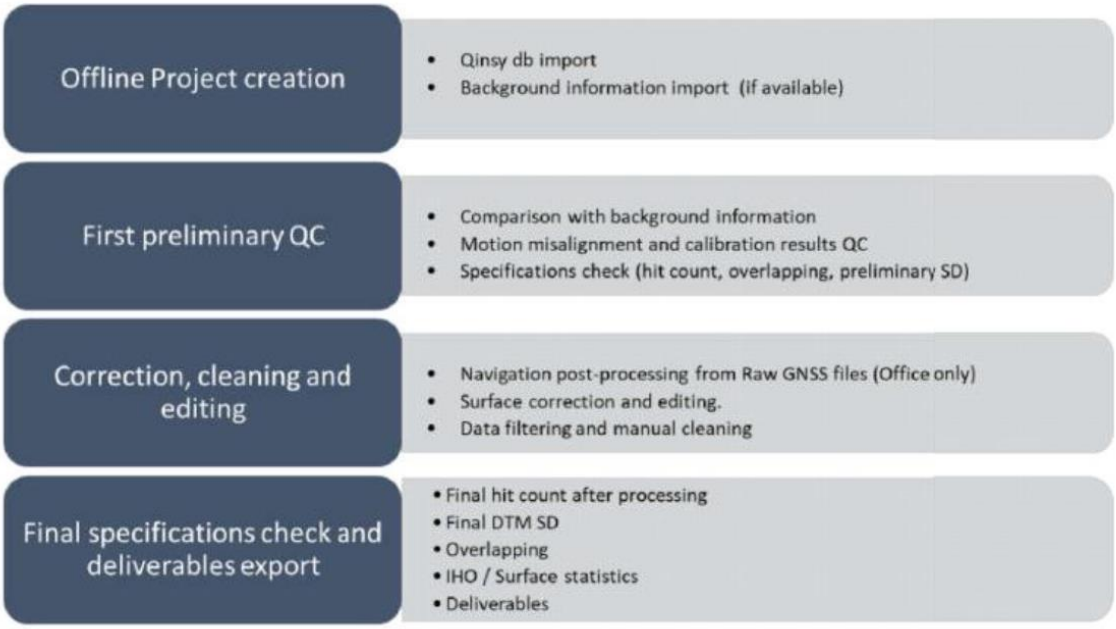

Figure 2-4: MBES bathymetry processing overview.

2.2. UHR SEISMIC

2.2.1. Data acquisition

UHR Seismic data was acquired using GSO 540-tip Sparker sled and Applied Acoustics CSP-N pulsed power supply unit as the acquisition source, interfaced with a Geometrics GEOEEL LH16 recording system and 48 channel UHR streamer. The first 24 channels of the streamer were at a 1m group interval and the remaining 24 channels at 2m. The streamer was kept at a depth of 1m by a head and tail buoy as well as 2 Digicourse 5011 levellers (birds).

Accurate positioning was collected using Modulus 101G GPS pods mounted on each towed system, sparker sled as well as head and tail buoys for streamer positioning.

The shot point interval for the survey was 1 m, giving a nominal fold of 36 when binning with a CDP spacing of 1m to keep the bins consistent with the variable channel spacing. True fold will vary around this value when real source and receiver positions are used rather than nominal geometry, according to variations in ship speed and feather angle changes between shots.

Table 3: UHRS operational parameters.

Parameter	Value
Active Streamer Length	75m
Number of channels	48
Group Length	Channels 1-24: 1 m
	Channels 25-48: 2 m
Target Tow Depth	1m +/-0.5m
Near Offset	~5-6m
Sample Rate	0.0625ms
Record Length	0.250ms
Shot Point Interval	1m
Source	Sparker – GSO – 540 tips
Target Source Tow Depth	0.3 m

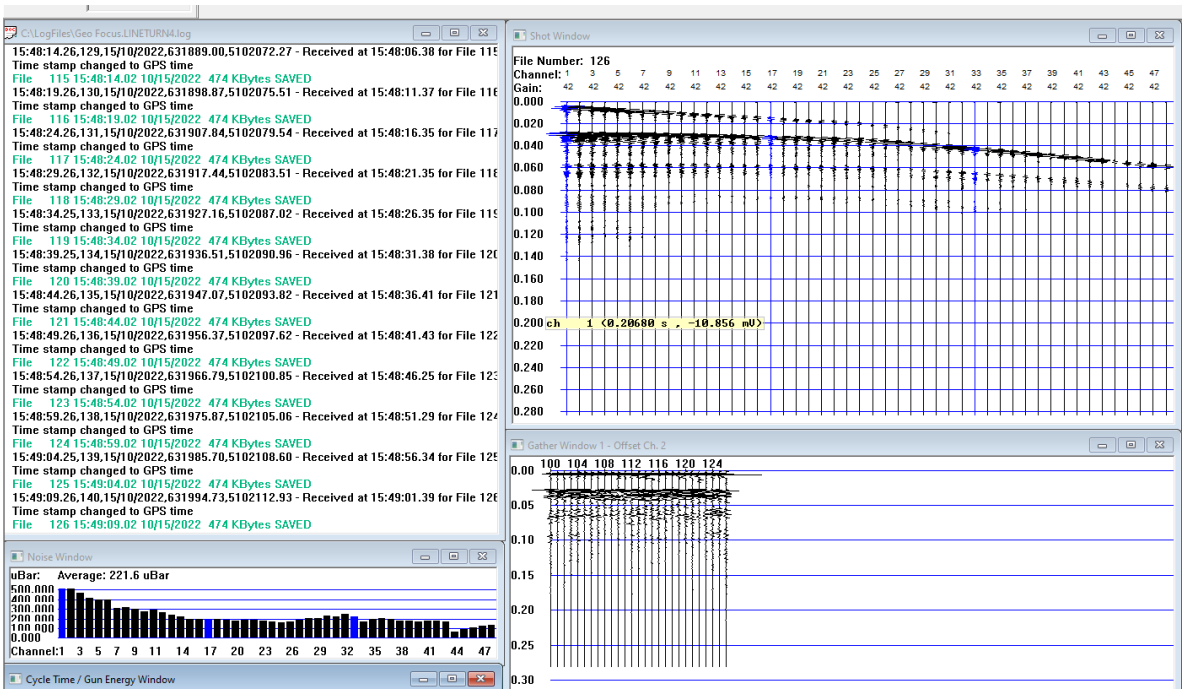

Figure 2-5: Screenshot from Geometrics LH16 software during UHR Seismic acquisition.

The guidelines followed by Tecnoambiente during the UHR Seismic data acquisition were the ones provided from TTS:

- IT-CM-17 Sparker Deployment Recovery, 2
- IT-CM- 34 Geoeel Instrument Verification Procedure
- IT-CM-35 Multichannel Seismic Streamer Deployment
- IT-CM-36 Multichannel Seismic Streamer Recovery
- IT-CM-37 Sparker Pulse Test Procedure
- IT-CM-38 LOTO Sparker Bangbox

These guidelines can be found in the quality plan document OLE_TEC_00004_IFE_rev02 - Quality Plan.

2.2.2. Data processing

Data processing and interpretation was performed within the OLE_AO7 area to a recorded length of 100 m sub-seabed for both OWFs and OSSs. This interpretation was done for evaluation of seabed and sub-seabed conditions.

The dataset was quality controlled offshore on board the vessel Situla by Peak Processing using a Linux based system with Landmark's ProMAX processing software.

The dataset was then made available to Peak Processing upon completion of the fieldwork. Final processing of the dataset took place ashore, and full details of the processing can be found in a dedicated seismic processing report.

Stacking velocities generated during the processing of the UHR data were used to help choose velocities in the time-depth calculation. Interval velocities were chosen based on sediment characteristics. For the interbedded sands and clays, as interpreted in AO7, an assumed seismic velocity of 1700m/s has been used. Within the bedrock, velocities increase to between 2000-2500m/s.

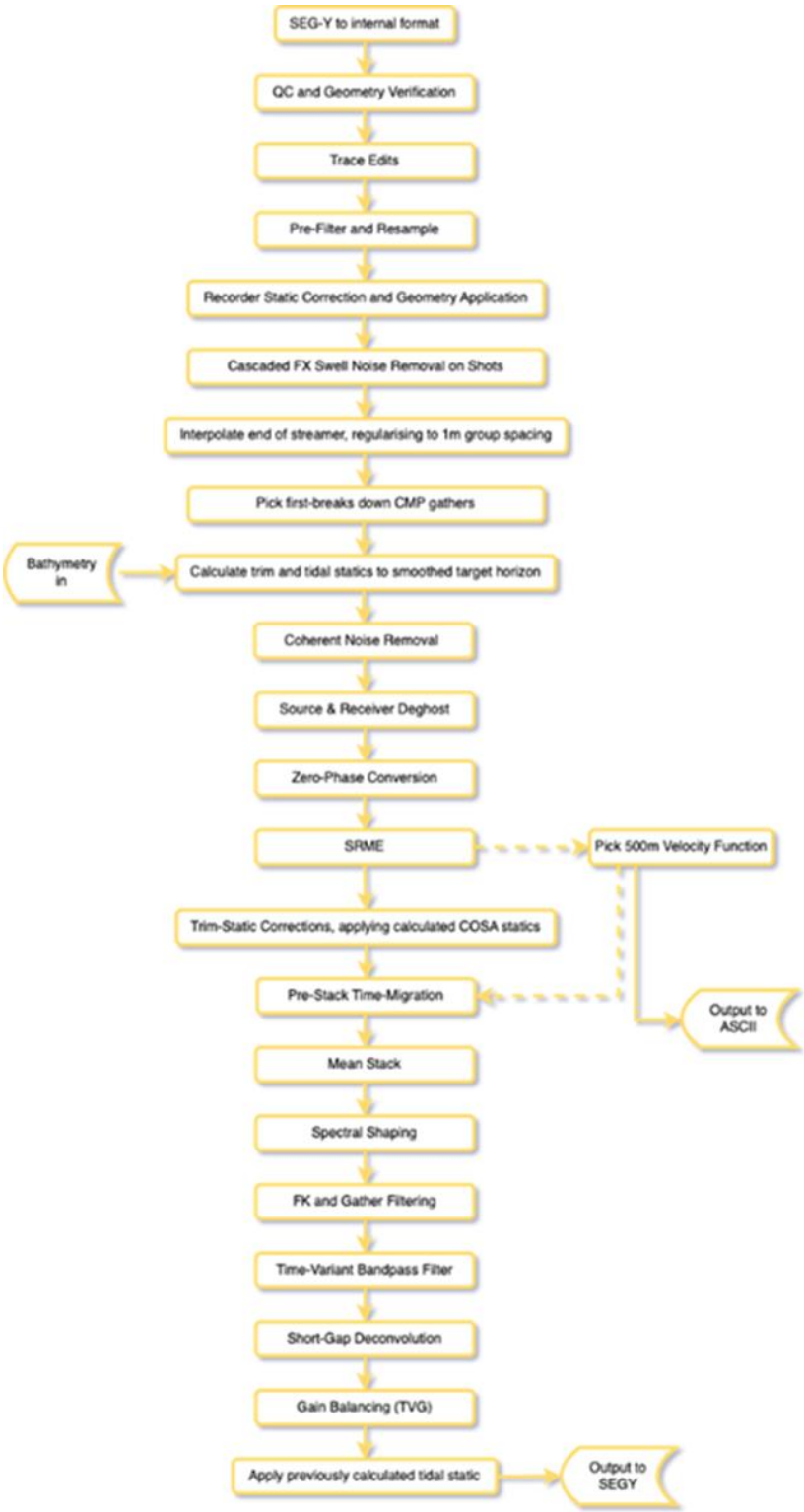

Figure 2-6: UHR Seismic processing overview.

For quality assurance, displays of the following were produced for each line with a copy provided to the client representative offshore, in addition to the Brute Stack SGY exported:

- Near trace
- Shot record examples (displayed every 100 shots)
- RMS Noise
- Spectral Analysis
- Offset QC checks, showing computed arrival time from offsets derived from GPS navigation data overlaid on top of the direct arrival in the data itself
- Velocity Semblance/Gather Example
- Brute Stack, annotated with trace fold header plot

As a summary, the evolution of the dataset can be seen in the following examples shown at three different stages of the processing:

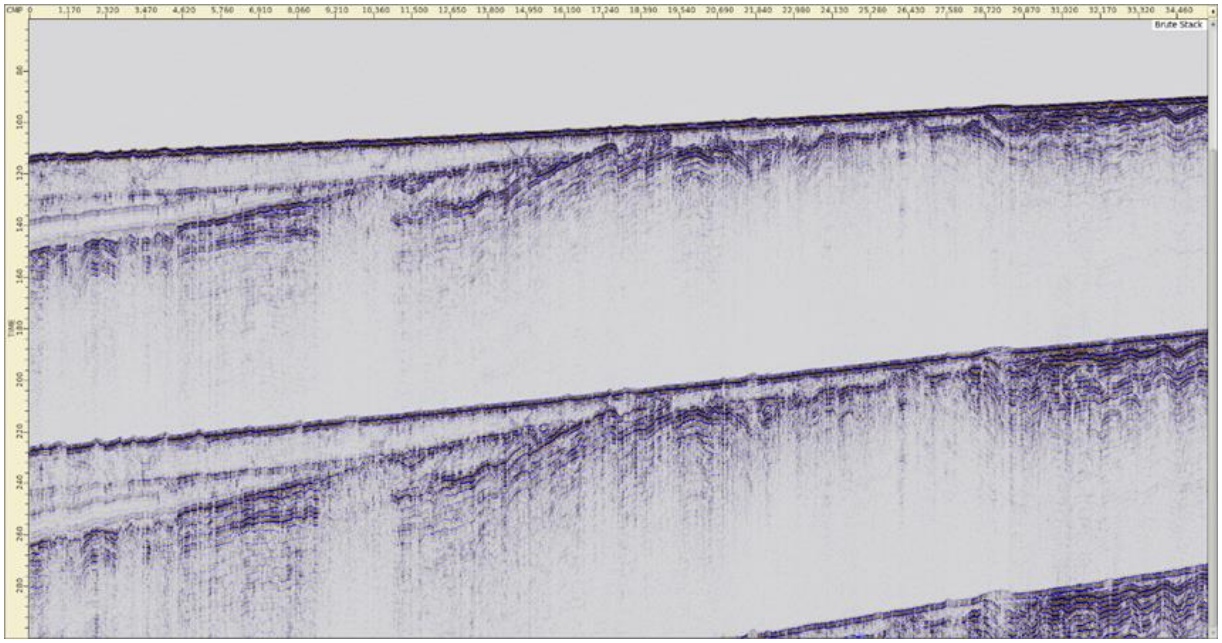

Figure 2-7: Minimum phase brute stack

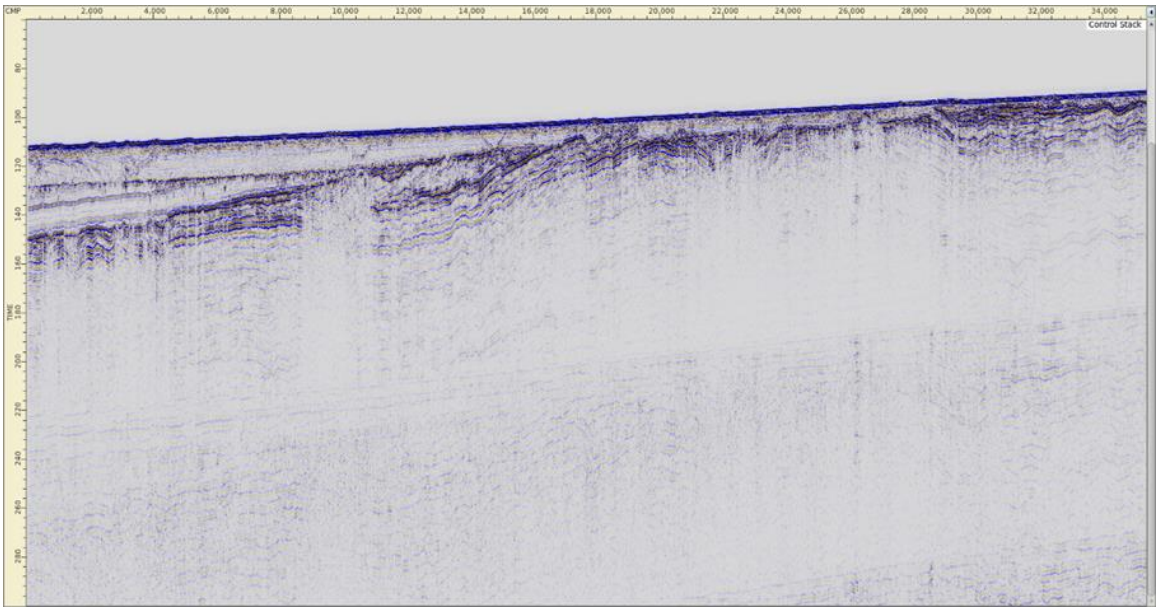

Figure 2-8: Zero-phase corrected control stack (Demultiple, Noise filtering, Deghost, Static Correction, Far Trace Mute & Pre-Stack Migration)

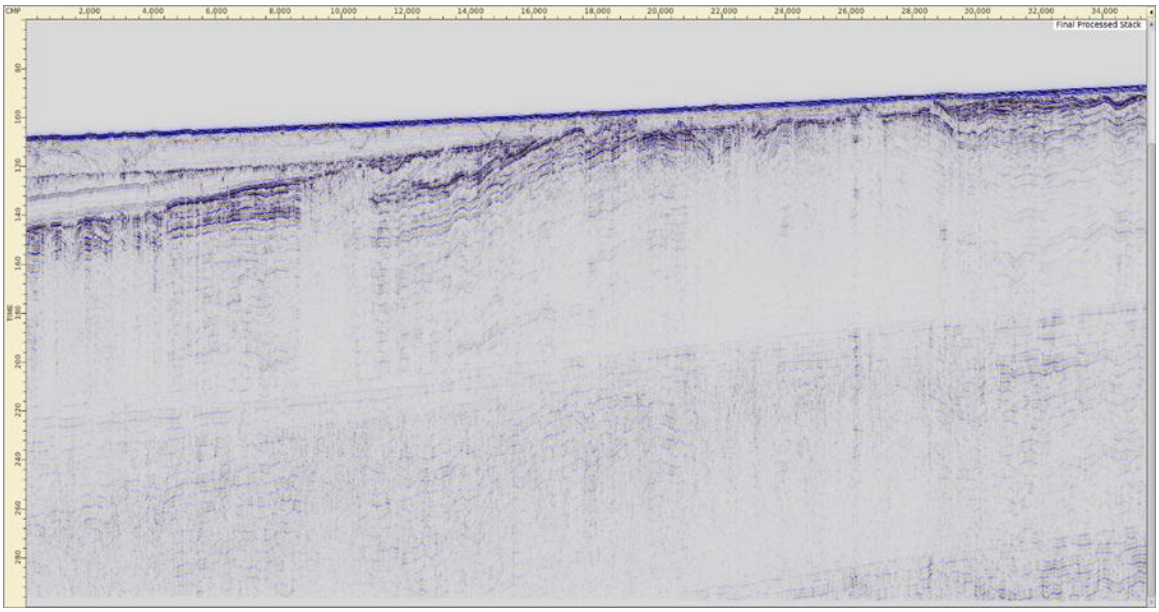

Figure 2-9: Zero-phase corrected final processed stack (Time-Variant Bandpass filter, FK filter, Gain balancing)

Interpretation was cross-checked for consistency at all crossline locations. Additionally, geo-hazards assessment was carried out focusing on the areas for planned shallow geotechnical operations. Heave corrections were applied after datum alignment with the MBES data.

3. RESULTS

3.1. BATHYMETRY

The detailed resolution of the bathymetry grid (Digital Elevation Model for seabed data following QUA-01-B GIS specifications) allows for enhanced visualization of depth and interesting seafloor features. The main use of the multibeam data is to reference the seismic profiles to the real seafloor (ZH Bathyelli v2 geoid).

In the acquired lines of the OLE_AO7 offshore windfarm survey area, the water depths range between -52.96 meters (ZH) in the shallowest part at the south-eastern region, to -83.45 meters (ZH) in the north-western region.

Bathymetric data from the vessel multibeam sensor has been processed into a 1 meter grid size bathymetry for all the acquired lines.

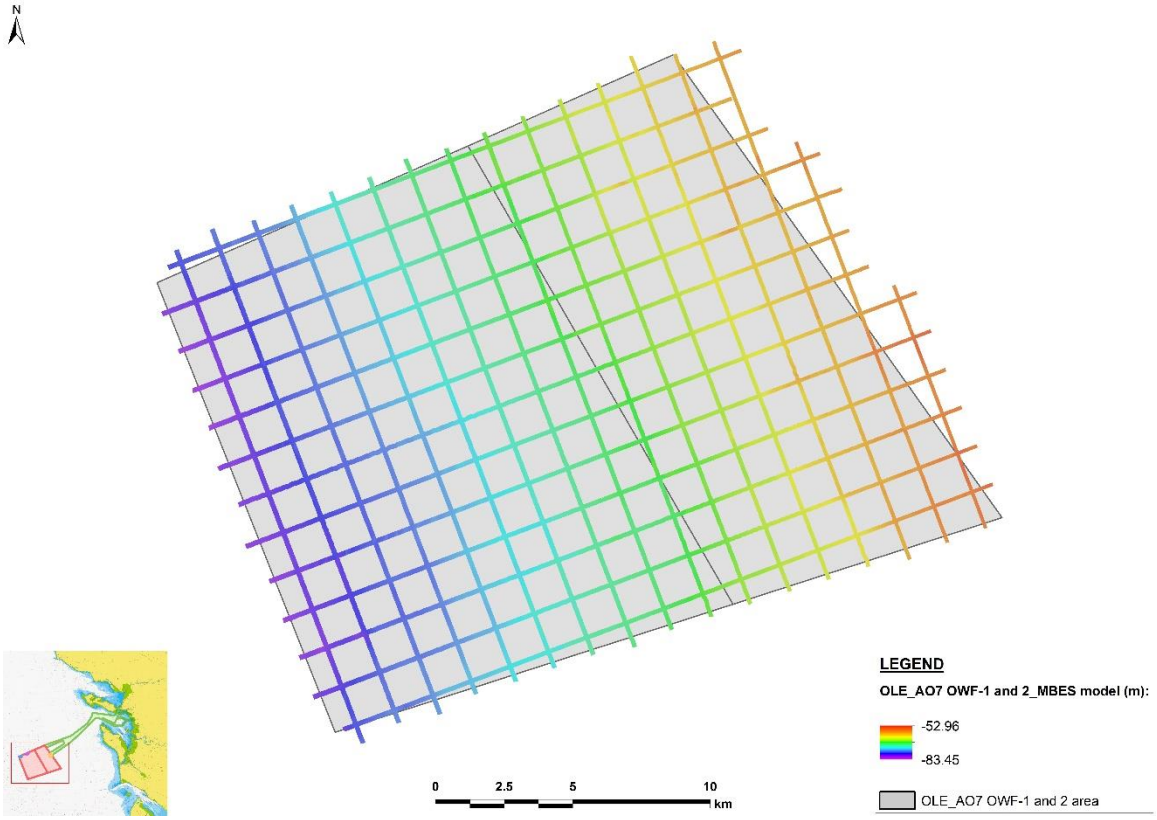

Figure 3-1: Bathymetric data grid model (1 x 1 m) for the OLE_AO7 OWF Parcs 1 and 2

3.2. GEOLOGY

3.2.1. Geological setting from background data

The survey area is in the Bay of Biscay, approximately 46km from the French coast. The Bay of Biscay is west of France, and north of the Iberian Peninsula. The survey area is on the continental shelf, north-west of the mouth of the Dordogne River.

The bay formed during the opening of the North Atlantic during the Late Cretaceous, with the rotation of the Iberian Peninsula. The nearshore continental crust shows evidence of complicated stress fractures, with basaltic oceanic crust further offshore. The Bay of Biscay has been subject to two well-differentiated continental margins: the Amorican Margin, to the north-east, and the North Iberian or Cantabrian Margin, to the south. The Armorican Margin

is a Mesozoic extensional passive margin mainly characterized by extensional faults, from the opening of the Atlantic Ocean. The area has also developed an east to west trending fault system, during the uplift of the Pyrenees. It consists of a Late Cretaceous - Cenozoic thrust system juxtaposing the continental crust of the Iberian Plate on top of the transitional-to-oceanic crust of the Bay of Biscay abyssal plain, westward, and on top of the thinned continental crust of the Landes Plateau, eastward.

The reworking of the sediments, as well as fluvial run off into the area give way to thin overburden sediments over the bedrock.

3.2.2. Geological sequence

Within the depth of interest (up to 30m below seabed), the OLE_AO7 OWF comprises a succession of probable Late Pleistocene sediments overlying Calcarenite. The interpretation is primarily based on the acoustic nature of the seismic data and unit boundaries marked by pronounced unconformities. Five coherent stratigraphic packages, over the first 30 m below seabed, are distinguished. Interpretation is limited to the Base Quaternary. One borehole is available within the OWF area, this extends to 60.4m below seabed (Table 4).

The location of this borehole means that most of the overburden sediments have not been sampled. Therefore, Units 1-4 are still primarily interpreted based on acoustic nature. Borehole results are time conversed using a velocity of 1700 m/s. This may be too slow for the bedrock component but is representative of the overburden sediments above the bedrock.

Table 4: Available borehole data from BH04.

DEPTH BELOW SEABED (m)	SEDIMENTS
0 to 6.5 m	Very loose to very dense SAND
6.5 to 10.15	Weak weathered CALCARENITE
10.15 to 12.25	Weak weathered SILTSTONE
12.25 to 23.90	Strong CALCARENITE

DEPTH BELOW SEABED (m)	SEDIMENTS
23.90 to 28.15	Weak weathered SANDSTONE
28.15 to 30.05	Fine to medium SAND
30.05 to 38.70	Weak weathered SANDSTONE
38.70 to 42.05	Strong SILTSTONE
42.05 to 48.60	Weak weathered CALCARENITE
48.60 to 54.20	Weak to strong LIMESTONE
54.20 to 58.75	Weak CALCARENITE
58.75 to 60.40	Weak to strong SANDSTONE

The shallow geology (to 30 m below seabed) within the OLE_AO7 OWF area has been divided into units based on the acoustic nature of the seismic data. There are four Quaternary units within the survey area.

Four horizons have been mapped within the OLE_AO7 OWF area, these represent bases of distinct sedimentary units. These surfaces are mapped based on the shared acoustic characteristics of the intervals they separate.

The youngest of these surfaces is the base of the Holocene sands (Base of Unit 1 – H05). The Holocene sand is subcropped by the Upper channelled unit, Unit 2 with H10 at its base; and the base of Unit 3 – H20, this unit is interpreted as predominantly sandy clay. This is subcropped by the area's oldest Quaternary unit, Unit 4, which is mapped with H30 at its base. Interpretation has generally been restricted to the Base Quaternary / Calcarenite, assuming a velocity of 1700m/s in the soft sediments. Isochores showing the sub seabed depths to H10, H20 and H30 are included as charts and as figures below.

Unit 1

Unit 1 is a thin unit with a flat reflector at the base and is interpreted as Holocene sand. The unit is up to 3m thick, acoustically quiet with a strong basal reflector. The exact extent of Unit 1 is uncertain due to the resolution of the UHRS dataset and the unavailability of SBP and SBF data: the interval is probably far more extensive than indicated in this report though as a thin veneer.

Where imaged, the base of Unit 1 (H05) has been mapped, although due to imaging limitations, an isochore map has not been produced. Instead, a ribbon plot showing the approximate extent of this unit is included as Figure 3-5.

Unit 2

Below Unit 1, Unit 2 has been interpreted across much of the site. Unit 2 is acoustically more ambiguous than the underlying sediments, although in the west there is quite often no strong reflector marking the base of the unit. Over large parts of the east of the area Unit 2 sediments directly overlay the bedrock.

Unit 2 contains downlapping reflectors indicating that the sediments were sourced from the east and laid down in the style of a delta; the sediments are younger to the east as well as upwards. This unit may represent sedimentary processes during times of lower sealevel when ancient rivers may have discharged sediment directly to this area.

In the west, the base of the unit is undulating, and occurs as an unconformity within a broadly similar sequence, indicating that, in this deeper water part of the area, sedimentary conditions were broadly similar over Unit 3 and Unit 2 at times. Unit 2 sediments are interpreted as silty clay. Unit 2 is illustrated in Figure 3-6 as a thickness below seabed and Figure 3-2.

Unit 3

In the west of the area Unit 2 is sub-cropped by Unit 3, an irregular package of acoustically quiet sediments interpreted to comprise silty clay. This unit is broadly similar to the Unit 2 overburden but pre dates Unit 2 and does not have similar downlap characteristics. Unit 3 has pronounced thickness variations due to the undulating nature of its upper surface, H10. The lower surface, H20, dips gently to the north-west.

Unit 4

Unit 4 is acoustically well layered and bedded parallel to the basal reflector. The unit is interpreted as a wedge shaped package of clay sediments, present only in the west of the

OWF area. The wedge is thickest in the west and pinches out in the east. The upper portion of the unit is well channelled, and relatively flat lying, the lower part of the unit is underlain by Calcarenite, which is gently dipping to the west. Within the unit, there are some higher amplitude isolated anomalies, both within the channels and within the surrounding sedimentary package.

Isochores illustrating the depth to the base of each of these units are illustrated in Figure 3-5 and Figure 3-9 respectively.

Unit 5

Unit 5, interpreted as Calcarenite, is observed underneath the Quaternary sequence. This unit is referred to as bedrock in this report. Unit 5 is heavily fractured and faulted in certain areas of the OWF. This is highlighted on the Isochore of the Base Quaternary in Figure 3-9, by the areas of tightly packed contours. The Calcarenite outcrops in the eastern half of the windfarm area, although, due to the resolution of the seismic data, the exact extent of the exposed bedrock may be better determined from the multibeam echo sounder data. An isochore of the Quaternary sequence is included as Figure 3-9, this is equivalent to the depth of the bedrock below seabed. Where the Base Quaternary is within 0.5m of seabed it is presumed too thin to determine and not included on the Isochore map.

The top of the bedrock is a strong truncation surface. It may have been subject to erosion during more than one Quaternary low stand. Further borehole data would aid in interpretation of the exact position of the top of the bedrock within the OWF; locally the transition between the Quaternary sequence and the bedrock is indistinct.

The borehole data (BH04 – Table 4), show a succession of Calcarenite between 6.5m and 10.5m below seabed, a thin band, up to 2m thick of siltstone, followed by a further succession of Calcarenite to 23.5m below seabed.

Some attempt has been made to interpret the extent of the thin band of siltstone (H40), as illustrated on Figure 3-4, although the distinctive character of this unit does not appear to be

widespread. Within the bedrock there are high amplitude dipping reflectors. These are interpreted as representing a change in lithology, or dipping strata.

Further geotechnical data would aid interpretation within the bedrock.

Figure 3-4 shows the UHRS data and interpretation at the BH04 well location.

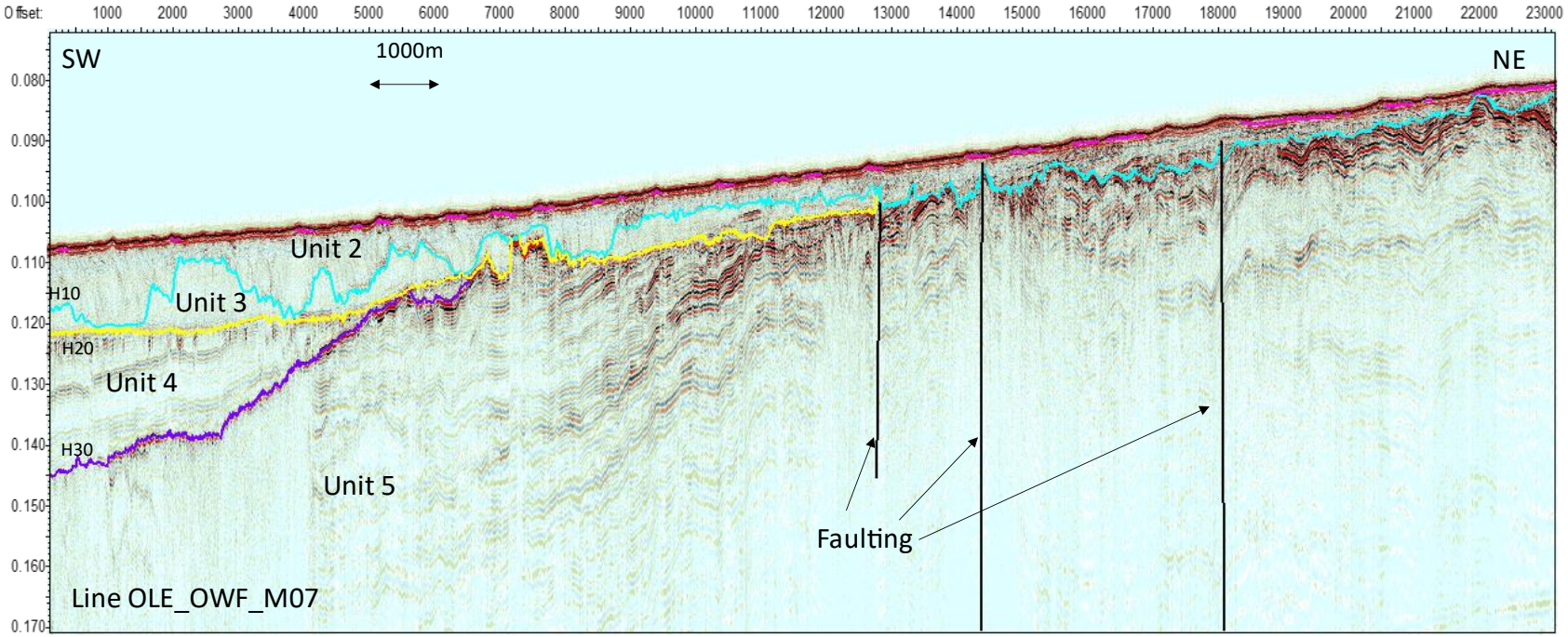

Figure 3-2: Line OLE_OWF_ M07.

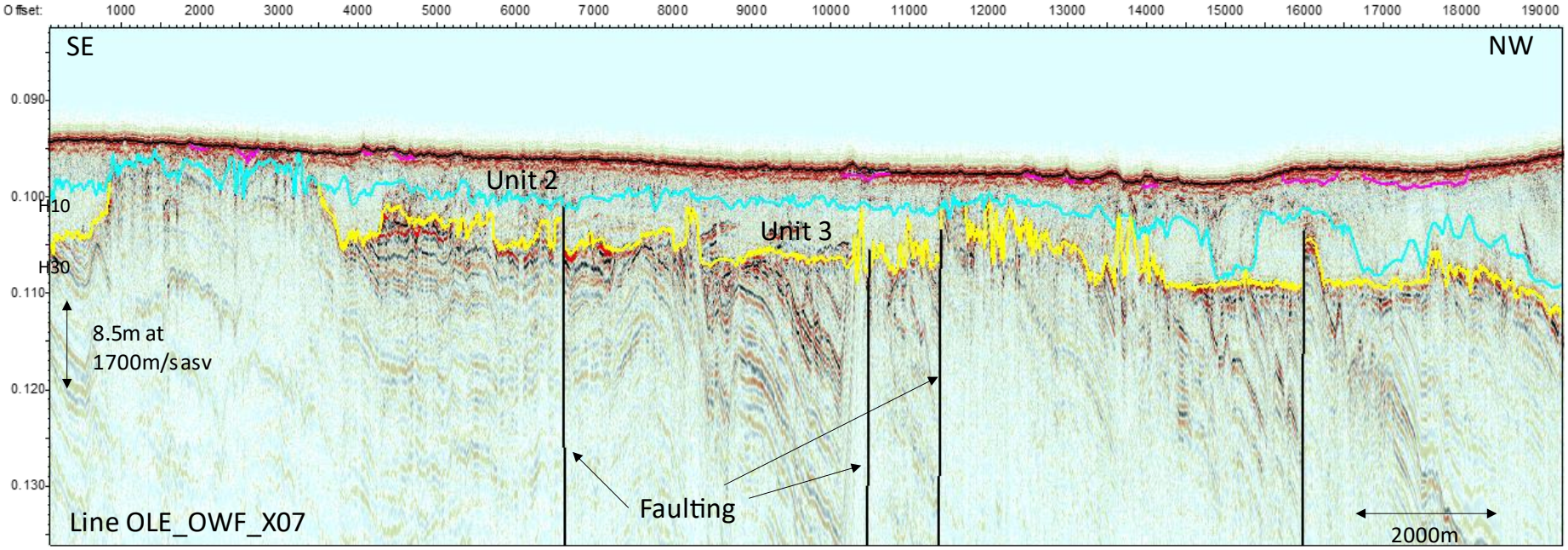

Figure 3-3: Line OLE_OWF_ X07.

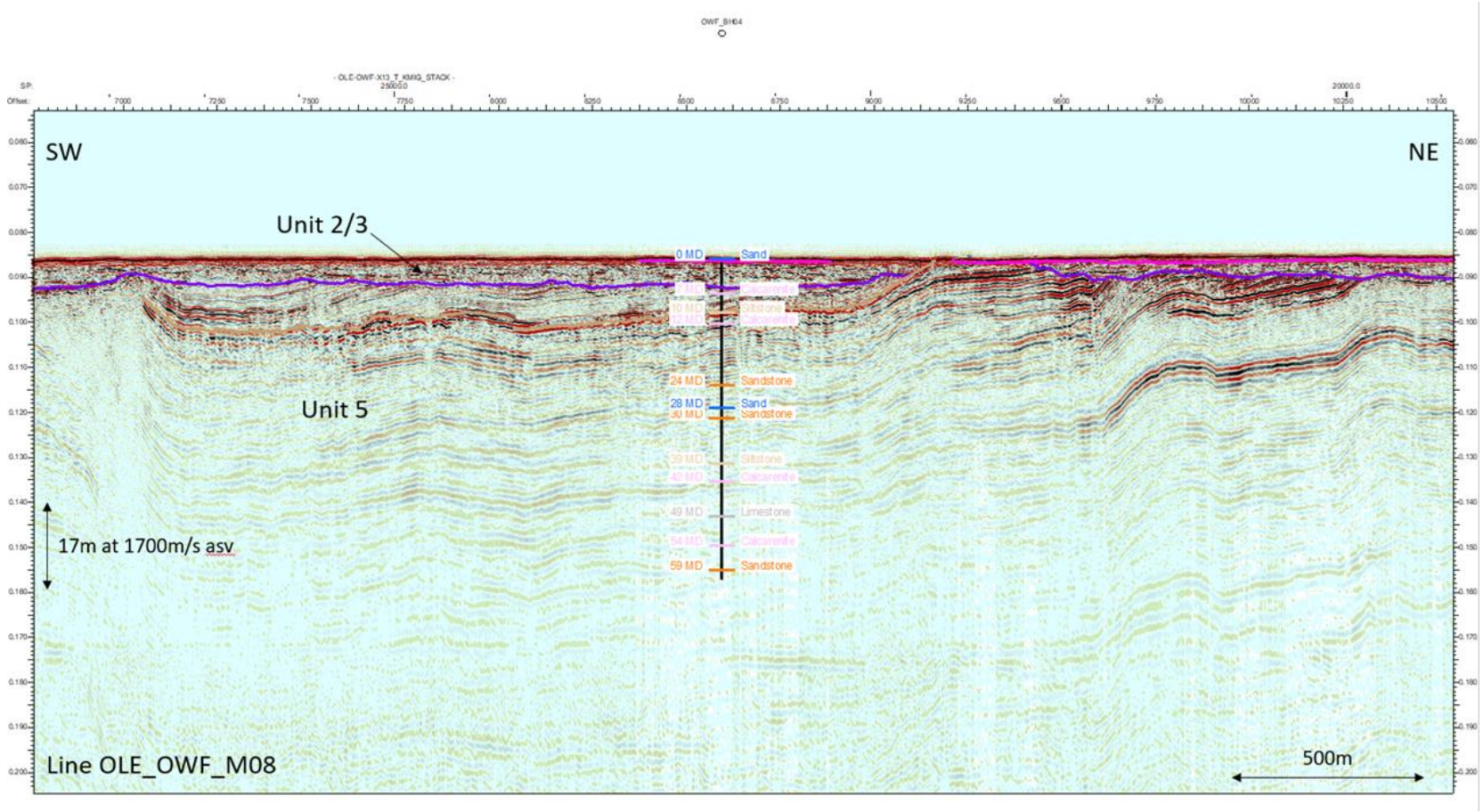

Figure 3-4: Data example through BH04.

Table 5: Shallow geological units.

Unit	Upper surface	Lower surface	Description	Depositional Environment
1	**Seabed**	**H05**	Predominantly a thin unit of sand, resolution of the data is too poor to fully determine the extent of the unit	Shallow marine, a drape of sandy lag deposit
2	**H05**	**H10**	Discontinuous reflectors, a package of sediment marking multiple events of erosional channels, depositional reworking and erosion. Acoustically chaotic. Evidence of unconformities, channelling. Strong normal phase reflector at the base of the unit. Predominantly sandy in nature, some coarser material, and occasional small clay beds may be present within.	Estuarine/lacustrine depositional and then terrestrially reworked
3	**H10**	**H20**	Restricted to the west of the area, in which are it can be similar in nature to Unit 2, acoustically quiet, little evidence of reworking of the sediments.	Laid down in deeper water than much of Unit 2, with a correspondingly reduced imprint of shallow water/terrestrial processes
4	**H20/H10**	**H30**	A wedge shaped unit, of parallel bedded reflectors, interpreted as a clay-prone unit.	Marine depositional environment.
5	**H10/H30**	**-**	A strong reflector marks the top of the unit. The unit is parallel bedded, though structurally disturbed. The sequence is probably well weathered at the top. This marks the bedrock. There are several faults within the Calcarenite. From the available borehole data the unit is thin, with siltstone underneath, although this change is not easily imaged on the UHRS data available	Ancient tropical marine.
6	**H40**		A strong reflector marks a change observed on the BH04 data to show a change from Calcarenite to up to 2m of Siltstone, followed by a further unit of Calcarenite, 6m thick. H40 is interpreted as the change into Siltstone.	Ancient tropical marine.

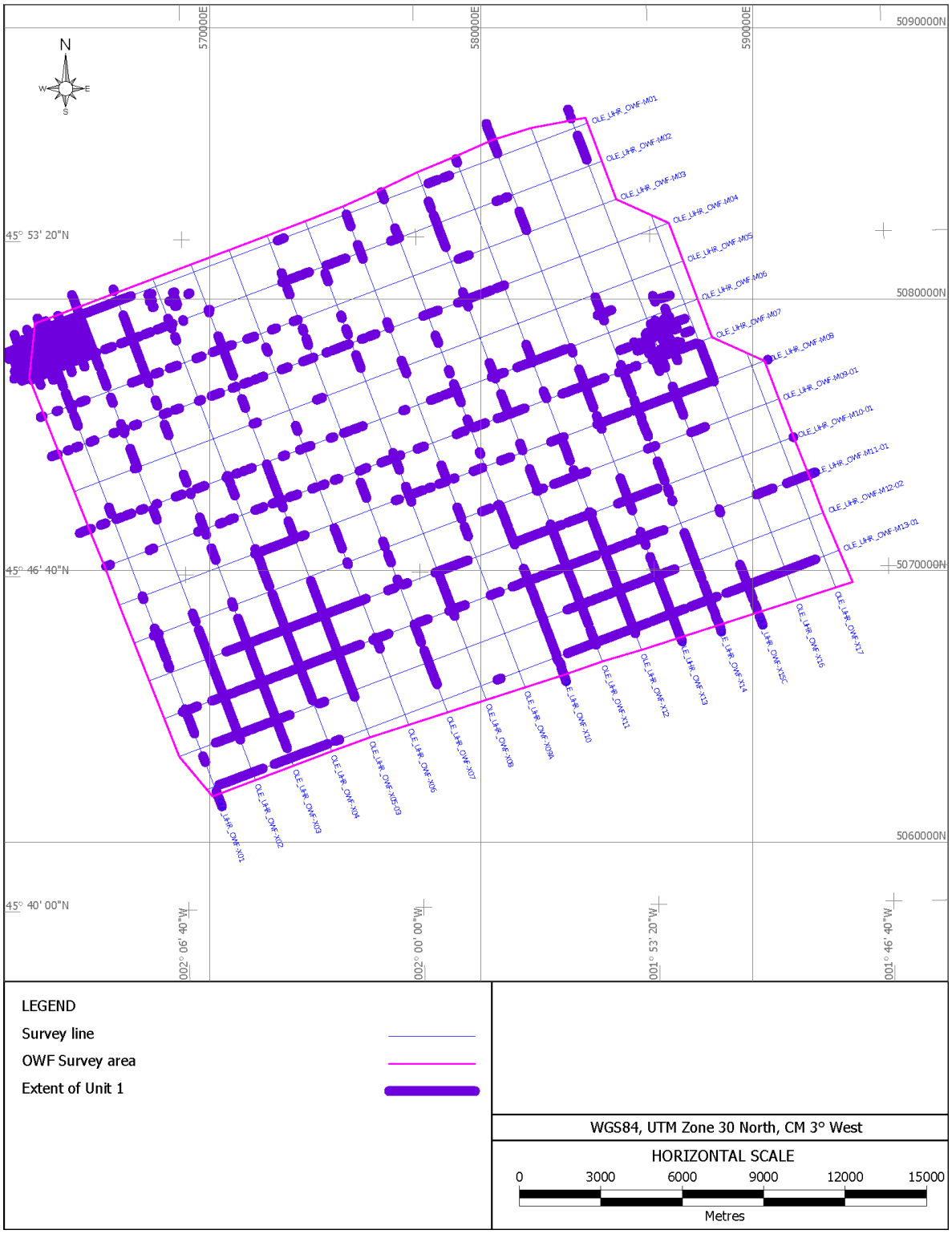

Figure 3-5: Ribbon plot of Unit 1 (H05)

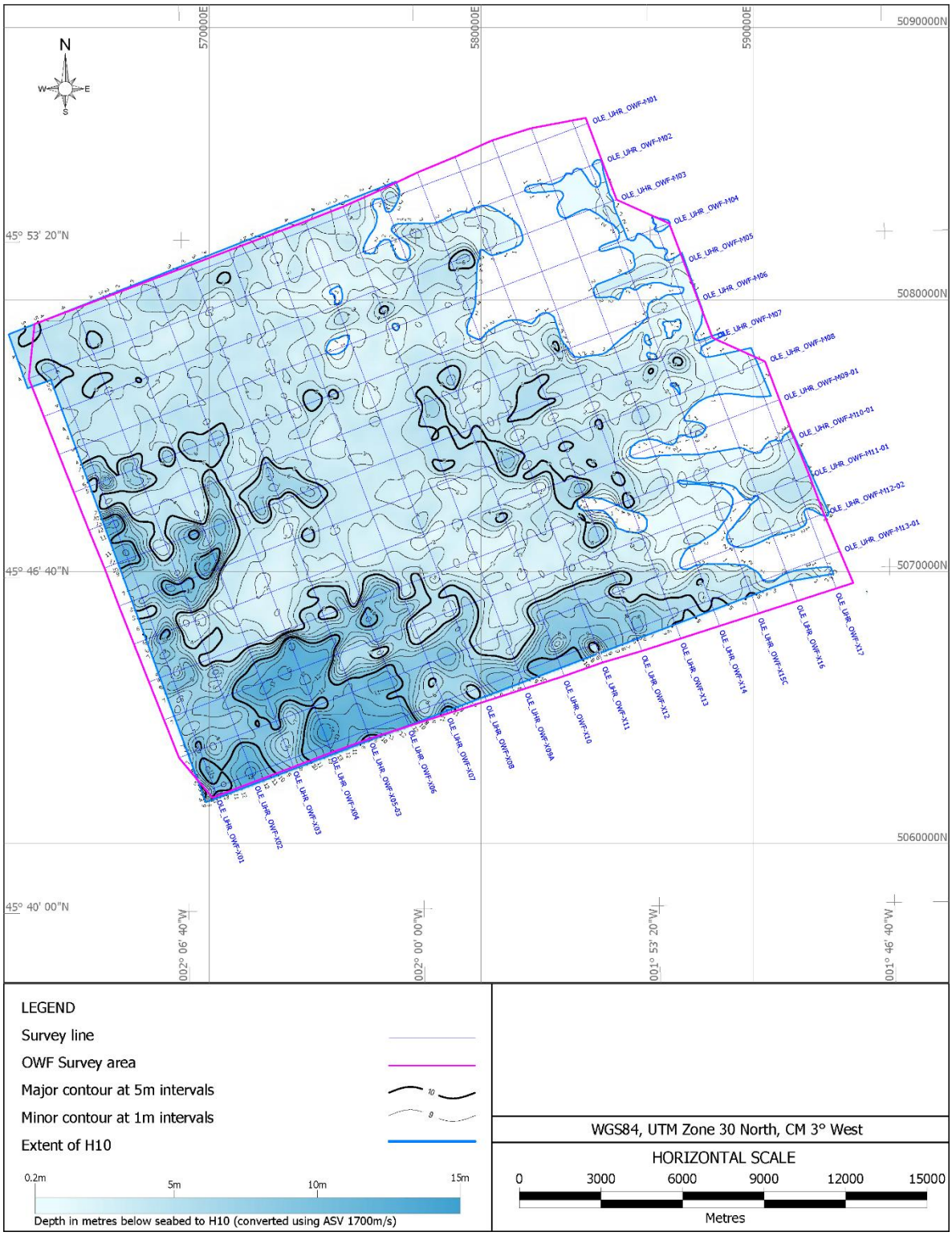

Figure 3-6: Isochore of H10, depth below seabed (base Unit 2).

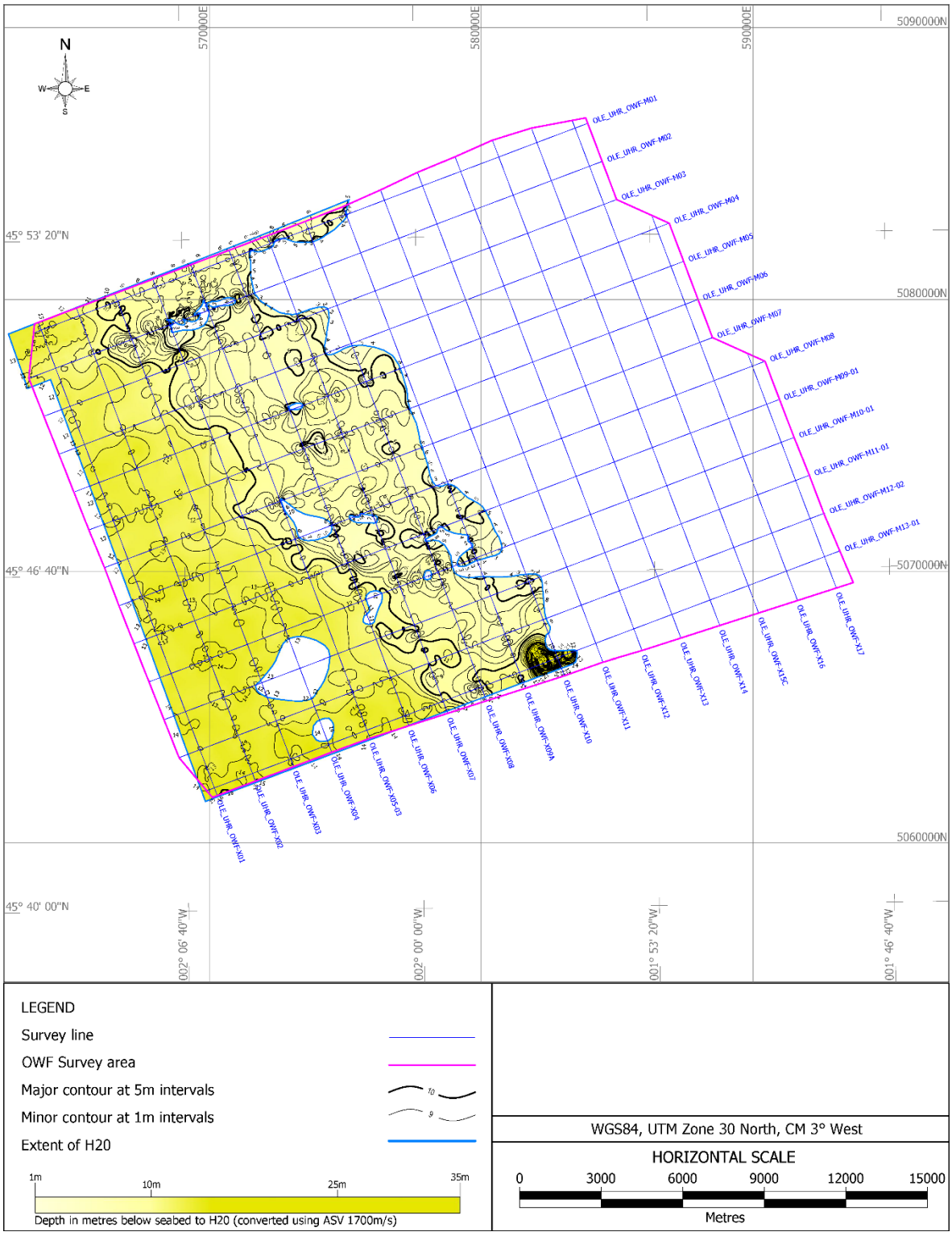

Figure 3-7: Isochore of H20, depth below seabed (base Unit 3).

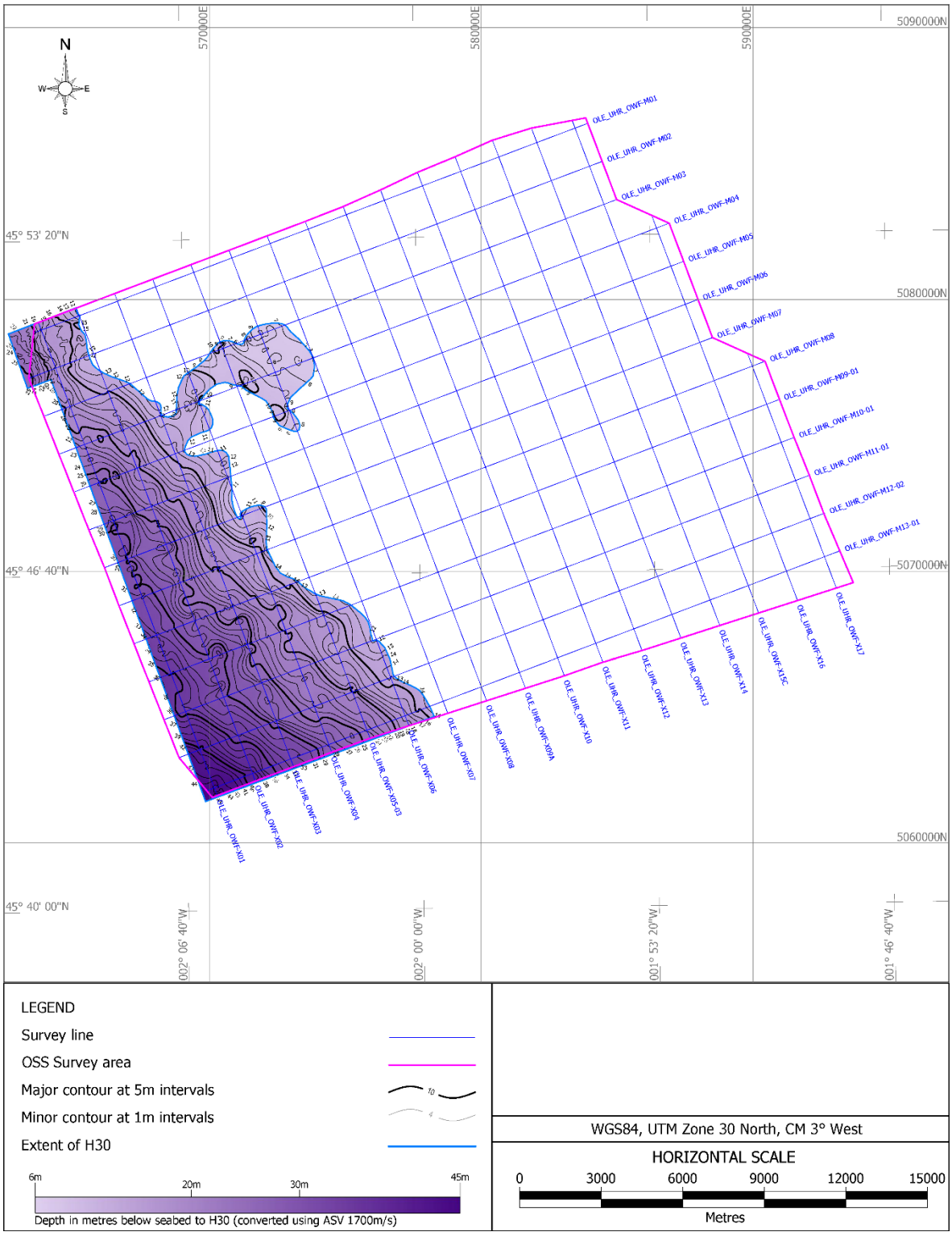

Figure 3-8: Isochore of H30, depth below seabed (base Unit 4).

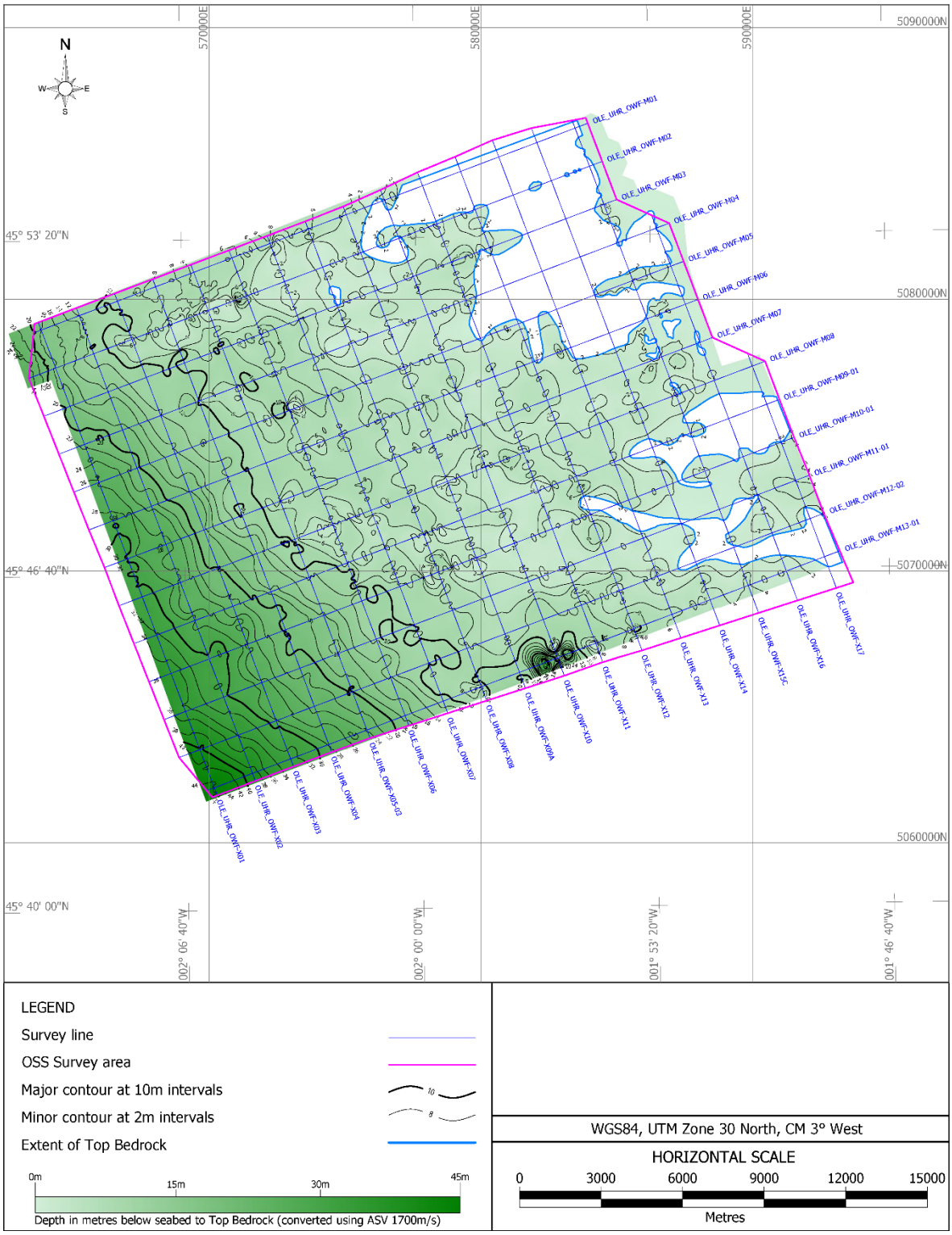

Figure 3-9: Thickness of Quaternary Sequence.

3.2.3. Geohazards

The UHRS data has been checked for evidence of any shallow geohazards that may affect the installation or operation of a wind farm. Constraints may relate to composition, distribution and variability of sediments (at the seabed and in the subsurface) within the first 30 m below the seafloor. Other constraints may relate to past or presently active geological processes, such as faulting.

A summary of geological conditions and potential constraints on infrastructure and engineering activities, applied to the OLE_AO7 site, is provided in (Table 5) modified after (Mellet, Long, Carter, Chiverell, & Van Landeghem, 2015).

Shallow Gas is present within the OWF area. Gas level 1 occurs within Unit 4 and interpreted to be biogenic gas contained within small channels. Unit 4 is only present in the western half of the survey area as shown on Figure 3-7. These gas hazards have been interpreted based on anomalous amplitudes, some acoustic blanking, and disturbance below. An example of the shallow gas within the survey area is illustrated in Figure 3-11.

Gas Level 2 has been interpreted as gas within the bedrock. One or two lines show a seismic character which it is difficult to interpret as anything else (Figure 3-13). Further borehole data would help, but it is expected that, if present, it would be occurring within the Calcarenite, Siltstone and Sandstone units identified within the available borehole (BH04), which could act as reservoir rocks, with the Quaternary sediments acting as a seal. The faults could be migration pathways.

The probability of these Level 2 anomalies representing gas is more difficult to assess than the shallower anomalies. The possibility that gas is present cannot be ruled out. There are areas where the seismic data exhibits acoustic blanking, interpreted to be due to the scattering of the acoustic signal over a highly irregular surface, or an area of weathered bedrock, or strong reverse phase high amplitude reflectors with a loss of frequency content beneath it, interpreted as a highly weathered surface, or a hard reflector. However, as gas is possibly present elsewhere, it would be advisable to treat these areas with caution and

the presence of gas cannot be ruled out. The location and extent of the interpreted gas hazards are shown on Figure 3-10.

The Calcarenite is faulted. Faults are widespread across the survey area. Figure 3-10 shows the faults as mapped on the UHRS data. They are predominantly near vertical faults with displacement of up to 4m, and although there is some agreement from line to line, tighter line spacing within the OWF would help to track the faults across the wind farm area. Figure 3-11 shows the locations of the main faults in plan view within the survey area. They are best imaged on the north-south orientated lines. These larger faults may have very significant displacement and may have a strike-slip component; the orientation of these faults suggest that they may be related to the opening of the Atlantic.

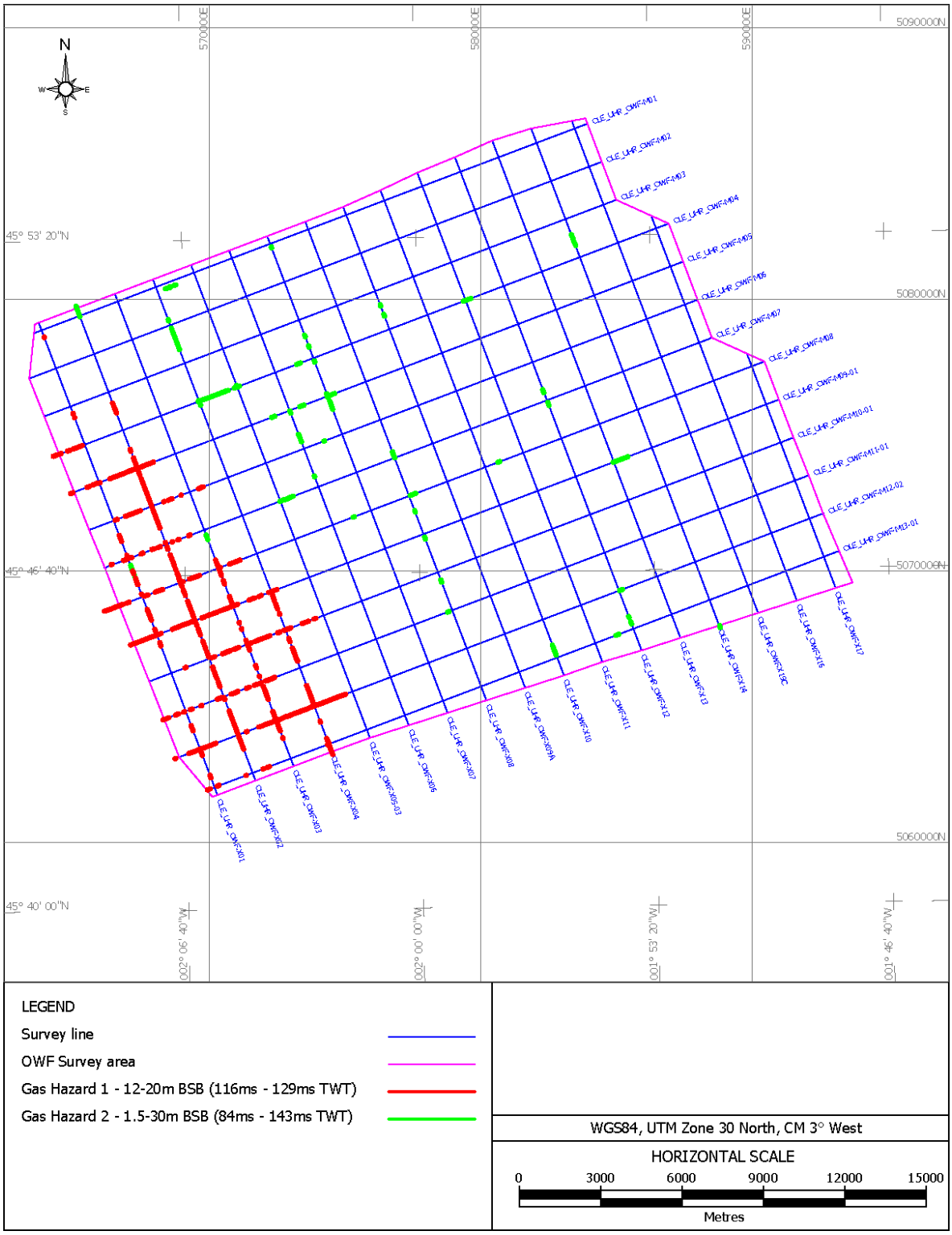

Figure 3-10: Gas hazards.

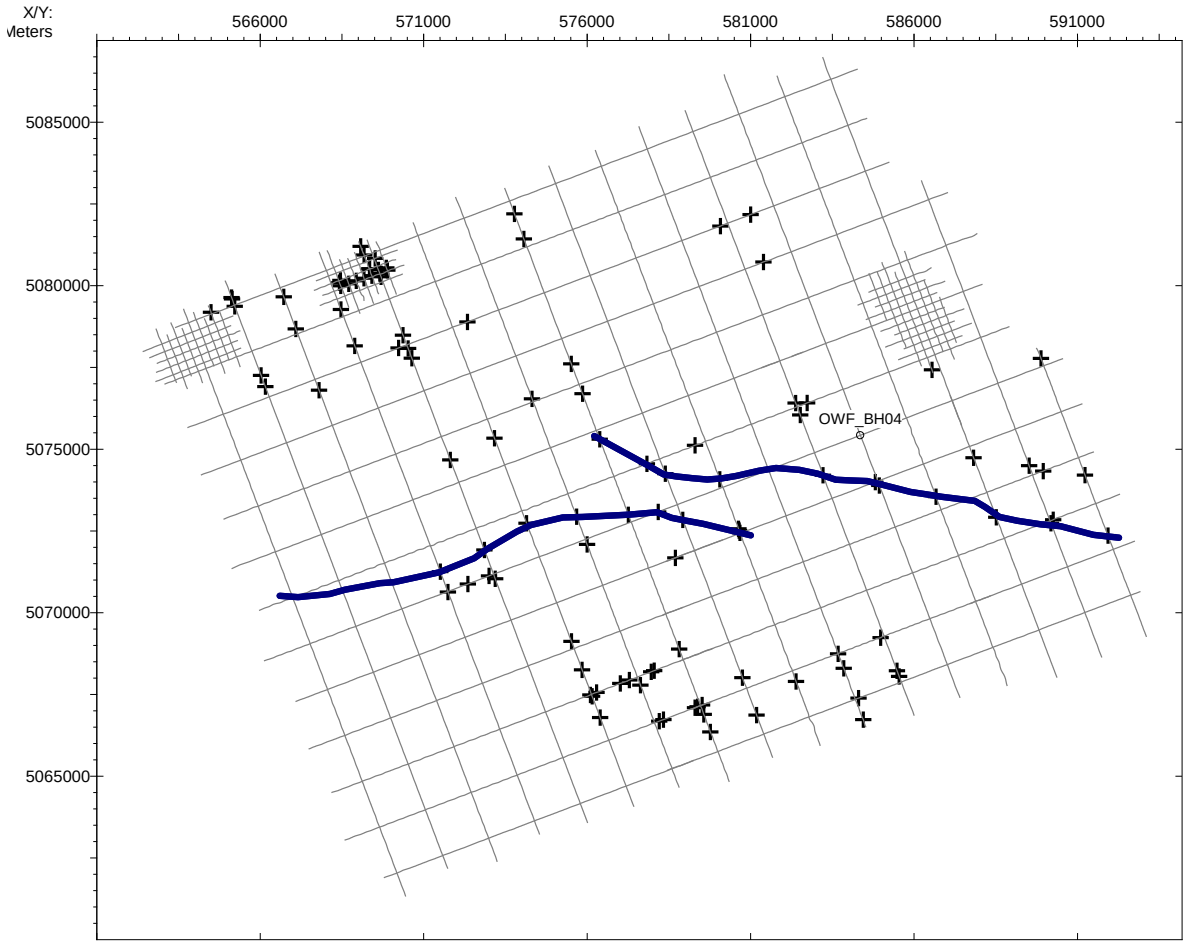

Figure 3-11: Illustrating the Main Faults within the bedrock.

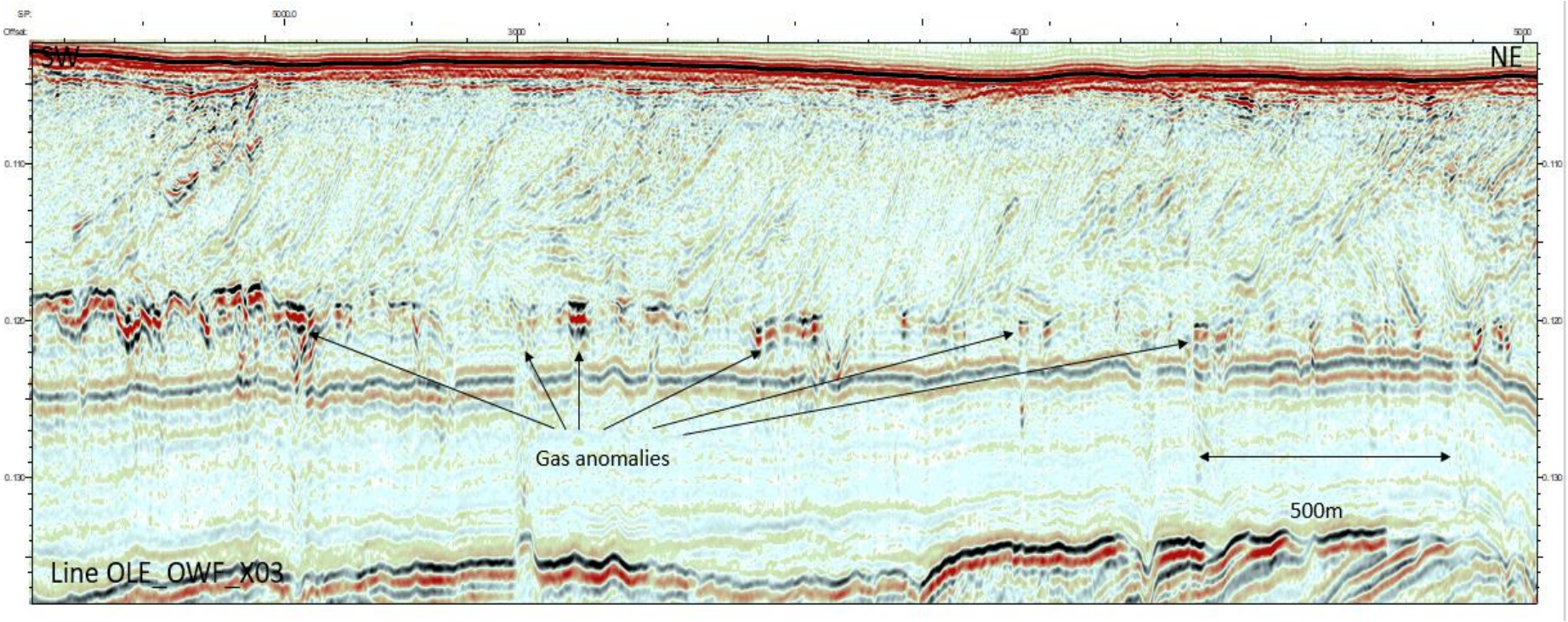

Figure 3-12: Example of gas anomalies (Gas Level 1).

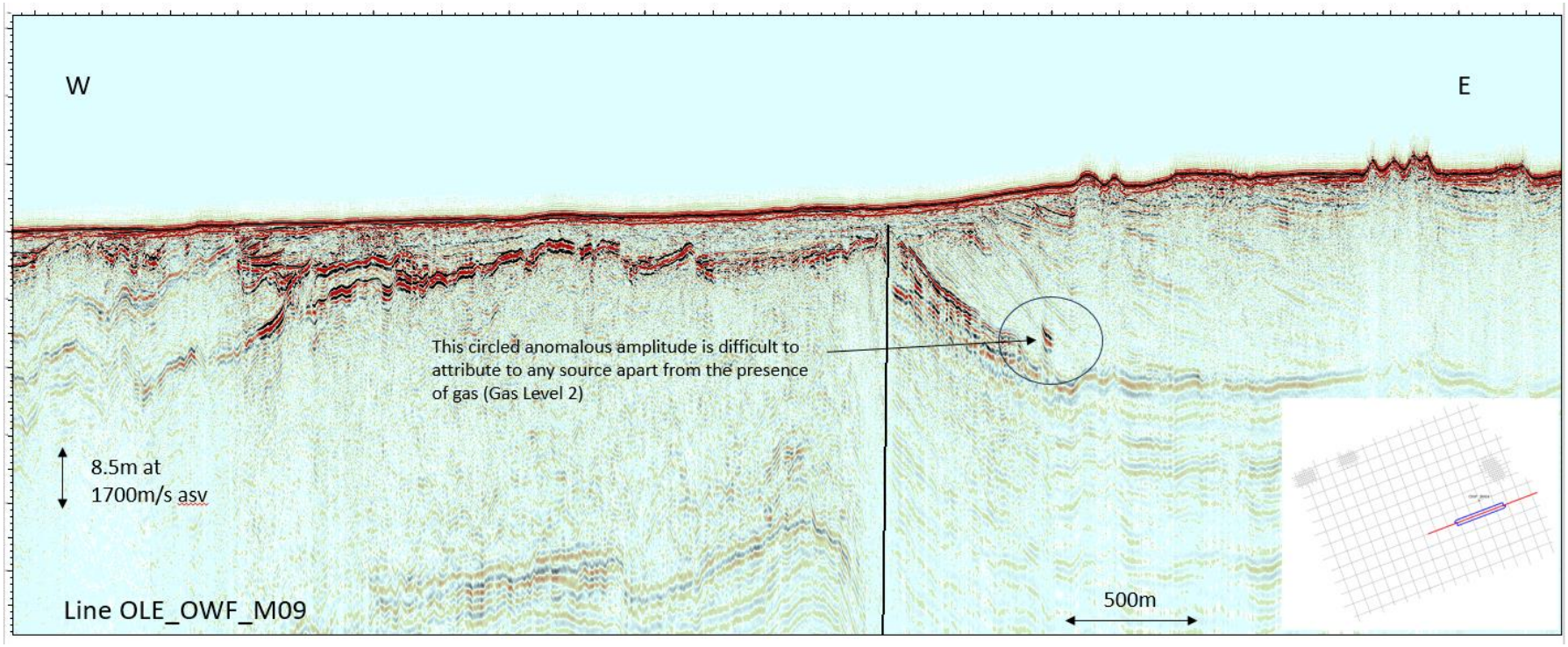

Figure 3-13: Example of gas anomalies (Gas Level 2).

Table 6: Geological characteristics / processes and potential constraints.

Geological characteristic / process	Potential constraint	OWF site
Seabed sediments		
Soft muds	Low strength means they will not bear large loads	Probable
Coarse lag (gravel to boulders) deposits	May be present below mobile sediment	Probable
Mobile sediment		
Migrating bedforms change topography (can create seabed features several metres height)	Can bury or expose structures or create a barrier to activities	Not evident
Mobile sediment can change sediment characteristics at seabed	Mobile sediment is constantly changing. Therefore, expect variation between samples taken from the same site at different times	Not evident
Bedforms can migrate in the opposite direction to that predicted from morphology and tidal residual	Do not assume sediment migration pathways from morphology. Repeat bathymetric surveys should be carried out	Not evident
Gas/fluid escape and MDAC		
Gas or fluid present in shallow subsurface	Can lead to blowouts when drilling	Gas is evident in the OWF, there is no evidence of the gas being under any considerable pressure
MDAC	Creates a hard substrate that is recognized as a special habitat that must be preserved	Not evident
Quaternary		
Variable sediment thickness	Locally, sediment thickness can change from thin (<5 m) to thick (> 50 m) over a short distance	Expected
Variable lithology (vertically and spatially)	Glacial processes rework and deposit sediments that are highly variable over large areas. Smaller and isolated features such as channels are not always mapped across the site. With the large line spacing some of the variations may not be incorporated into the interpretation	Expected
Heterogeneous sediment composition	Sediments are typically glacially diamict which are poorly sorted mixtures of silt, sand, gravel, and clay. Diamicts can be interbedded with sands	Probable

Geological characteristic / process	Potential constraint	OWF site
Bedrock		
Bedrock outcrop at seabed	Provides a hard substrate for emplacement of seabed infrastructure	Calcarenite outcrops at seabed within the OWF area.
Faulting	Active faults are susceptible to ground surface ruptures that can compromise infrastructure; seabed forms that indicate pre-existing seabed instability, surface displacements, or fluid escapes are conditions that pose risk to infrastructure; Sub-surface fault zones may provide preferential conduits for gas migration, or may be hydraulically active during (or shortly after) earthquakes	The Calcarenite is faulted

The depth values were converted from time (TWT) using sound velocity of 1700 m/s in sediments and 1510 m/s in the water column.

3.2.4. Conclusions and recommendations/comments

Horizons were mapped to define units of shared sedimentary characteristics based on acoustic nature and known geology and environmental conditions during the time of deposition from background material. These have been illustrated as depth maps to show rough sedimentary thicknesses and assist with a ground model. The sediment types and any hazards present were mapped.

Gas is interpreted within Unit 4. The gas sits primarily within channels and appears as occasional isolated amplitude anomalies within the unit. There is evidence of disturbed sediments below. The most probable source of the gas is biogenic matter. Gas is also interpreted with the Unit 5 bedrock. There is uncertainty over the characteristics of this deeper gas.

Further data acquisition could improve the knowledge and confidence of the area's geological constraints.

1. Additional high-resolution seismic data at a closer line spacing to improve spatial mapping of stratigraphic units.

2. Acquire sidescan sonar and sub bottom profiler data to integrate with multibeam bathymetry and backscatter data.
    a. A detailed seafloor mapping with sidescan sonar data will identify potential natural and anthropogenic seafloor geohazards.

3. Acquire repeat multibeam bathymetry and backscatter data during sidescan sonar data acquisition.
    a. Use this comparative multibeam bathymetry data to assess potential for sediment mobility.
    b. Although a recent study concluded that sediment mobility is not apparent at the OLE_AO7 site, monitoring for its potential could be beneficial for long-term development planning.

4. Acquire basic seabed ground-truthing geotechnical data (e.g., grab samples) to confirm the variable seafloor composition imaged by side scan sonar data.

4. REFERENCES

Barrie, J. V., & Conway, K. (2014). Seabed characterization for the development of marine renewable energy on the Pacifi c margin of Canada. *Continental Shelf Research*, 45-52. doi:http://dx.doi.org/10.1016/j.csr.2013.10.016

Chaumillon, E et al. (2008). Incised-valley morphologies and sedimentary-fills within the inner shelf of the northern Bay of Biscay. Journal of Marine Systems, Elsevier, 2008, 72 (3-4), pp.383-396. 10.1016/j.jmarsys.2007.05.014.

Grosdemange, D., et le Tixerant, M. (2022). Etude bibliographique sur la geologie et elaboration du modele geologique au droit d'Oleron.

Huerta, P. et al (2010). Seismic stratigraphy of the Vendean-Armorican platform of the French Atlantic shelf: new insights into the history of the North Atlantic ocean. Bulletin de la societe Geologique de France.

Mellet, C., Long, D., Carter, G., Chiverell, R., & Van Landeghem, K. (2015). Geology of the seabed and shallow subsurface: The Irish Sea. *British Geological Survey Commissioned Report*, 52.

Weber, M. (2004). These par Morphologie, architecture des depots, evolution seculaire et millenaire du littoral Charentais. Apports de la sismique reflexion combine a des suivis bathymetriques et validee par des vibrocarottages

Ziegler, P. (1990). *Geological atlas of Western and Central Europe.*

APPENDIX I – CHARTING

CHART NUMBER	CHART TITLE
1	A07_OWF_BATHYMETRY
2	A07_OWF_GRADIENT
3	A07_OWF_HAZARDS
4	A07_OWF_ISOCHORE_H10
5	A07_OWF_ISOCHORE_H20
6	A07_OWF_ISOCHORE_H30
7	A07_OWF_ISOCHORE_Bedrock.
8	A07_OWF_PROFILE_M08_PT1
9	A07_OWF_PROFILE_M08_PT2
10	A07_OWF_PROFILE_M08_PT3
11	A07_OWF_PROFILE_X08_PT1
12	A07_OWF_PROFILE_X08_PT2

APPENDIX II – PROCESSING AND INTERPRETATION REPORT

UHRS Seismic Processing Report

PEAKPROCESSING

OLE_AO7 Area
UHRS Seismic Processing Report

Document Reference	PP2022-669 – UHRS Seismic Processing Report	
Issue Date/Version	17th July 2023	Version: 1
Client	Tecnoambiente	
Project Name	**OLE_AO7 Area Offshore Windfarm**	
Location	Gulf of Gascogne, Bay of Biscay, Offshore France	
Document Author	Tom Harrison	
Approved By	Neil Wakefield	
Reason for Issue	Draft issue	

Contents

1. Version Control 3
2. Seismic Data Processing 4
2.1. Introduction 4
2.2. Processing Sequence and Testing 8
3. Seismic Processing Flow Chart 21
4. Deliverables 22
5. SEG-Y EBCDIC Header Examples 23
5.1. UHR2D Migration Stack EBCDIC Header Example 23
6. Line Listing 24
6.1. OLE_AO7 Offshore Windfarms – UHR2D Survey Lines 24
6.1.1. OWF Lines 24
6.1.2. OSS-1 Lines 26
6.1.3. OSS-2E Lines 27
6.1.1. OSS-2W Lines 27

Figures

Figure 1 Location Map of survey areas 5
Figure 2 Full survey grid for all acquired lines 8
Figure 3 Shot record examples of raw shots before resampling (left/blue) and after pre-filter and resampling (right/red) 9
Figure 4 Frequency analysis of raw shots before resampling (left/blue) and after pre-filter and resampling (right/red) 9
Figure 5 Brute Stack 10
Figure 6 Stack example sub-section before denoise (left), after denoise (centre) and difference (right) 11
Figure 7 Sub-Section of Brute Stack, zoomed horizontally, showing trace fold header plot and irregular fold of cover 11
Figure 8 Selection of shots before interpolation (left) and after interpolation (right) 12
Figure 9 Stack example following interpolation to regularise channel spacing – nominal fold of is-36 12
Figure 10 CMP examples (x3) before (left), and after (right), residual static correction with water velocity NMO applied 13
Figure 11 Stack subsection before (left), and after (right), residual static correction 14
Figure 12 Stack subsection before (left), after (centre), and difference (right) with further denoise 14
Figure 13 Example shot records and corresponding spectra before (left/blue) and after (right/red) further denoise (lines in spectral plot sit nearly on top of each other) 15
Figure 14 Stack subsection examples before (left) and after (right) denoise and designature 16
Figure 15 Example shot records and corresponding spectra before (left/blue) and after (right/red) deghost and designature 16
Figure 16 Subset stack examples before (left), after (centre) and difference (right) of SRME application 17
Figure 17 Velocity picking example with semblance display (left), representative gather (centre) and stack with velocity picks and overlay (right) 17
Figure 18 Stack example at PSTM stage 18
Figure 19 Stack subsection example at PSTM stage, zoomed over the shallow section 18
Figure 20 Example stack below seabed of brute stack (left) and final stack (right) 19
Figure 21 Example stack subsection with brute stack (left) and final stack (right) 20
Figure 22 Processing Sequence Flow Diagram 21

1. Version Control

DATE	VERSION	CHANGE
17th July 2023	1	First issue for client review

2. Seismic Data Processing

2.1. Introduction

The dataset was quality controlled offshore on board the vessel 'Situla' by Peak Processing using a Linux based system with Landmark's ProMAX/SeisSpace processing software. The dataset was then made available to Peak Processing upon completion of the fieldwork with the processing finalised using Shearwater Reveal version 5.1 on a small cluster.

Acquisition of the UHR seismic work scope at the Offshore Wind Farm areas was completed in a single campaign between May and June 2023. Data was then sent to the Peak Processing offices, with the seismic processing completed between June and July 2023.

The objective was to provide a UHR seismic dataset for use in geological interpretation of the offshore wind farm survey areas. Specific aims were to define the shallow subsurface geology and any potential geohazards such as shallow gas, both generally across the sites and at proposed geotechnical locations.

The dataset comprised:

OLE_AO7 Area Offshore Windfarm and OSS locations:

AREA	SURVEY LINES ACQUIRED	TOTAL LENGTH OF LINES PROCESSED
OWF	39	523.30
OSS-1	16	98.83
OSS-2_E	10	60.39
OSS-2_W	13	78.97
TOTALS	78 UHRS lines	761.49 km

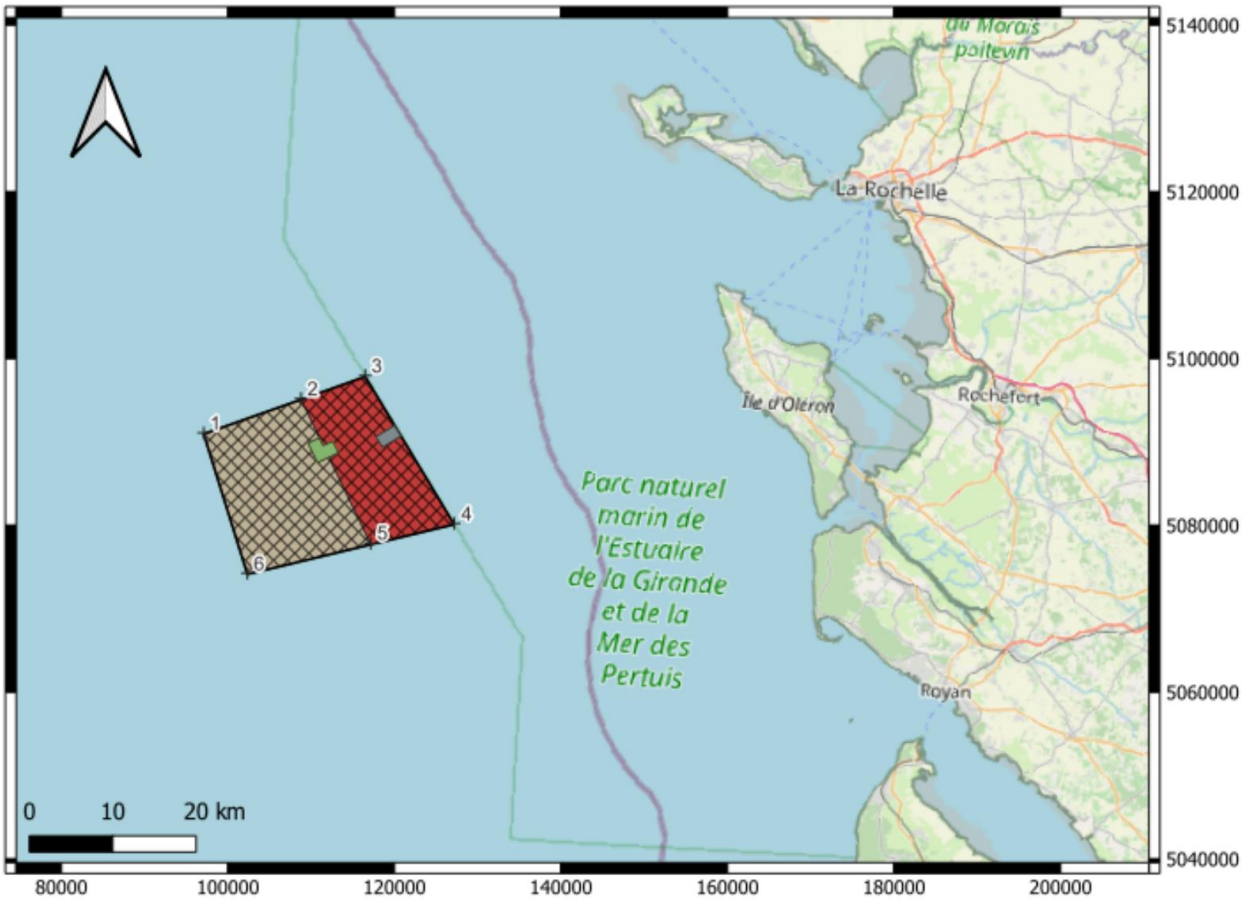

Figure 1 Location Map of survey areas

The UHR2D lines were acquired with a 0.3s record length. A single-sled sparker source that fired at a 1m interval was used together with a receiver array that consisted of a 48-channel streamer with the first 24 receivers spaced at 1m and the last 24 receivers spaced at 2m. The recorded sample interval was 0.0625 msec.

Further acquisition parameters are summarised in the table below:

RECEIVER PARAMETERS	VALUE
Streamer Type	Geoeel
Number of streamers	1 (2D)
Number of channels	48
Channel Spacing	Channels 1-24: 1m, channels 25-48: 2m
Active length	72m
Streamer Tow Depth Target	1m
Streamer Tow Profile	Flat
Centre of source to centre of channel 1 distance	Approximately 8.1m
Maximum target feather angle	12 degrees

SOURCE PARAMETERS	VALUE
Source Type	GSO 540 Sparker
Number of sources	1 (2D)
Number of levels	1
Source power settings	1200J
Source Tow Depth Target	0.5m
Shot Point Interval	1m

RECORDER PARAMETERS	VALUE
Recorder Type	Geometrics Geoeel LH16
Format	SEG-D
Sample rate	0.0625ms
Record Length	0.3s
Positioning System	Qinsy
DGPS Positioning	DGPS

The raw field data was recorded in SEG polarity (positive acoustic pressure written as negative numbers on tape).

QC was provided for each line sequence and made available to the offshore client representative. All the data acquired were passed through a QC sequence that incorporated the following steps as a minimum:

1) Reading the raw data onto the system, data from every line.

2) A selection of shots in their entirety were displayed and inspected from each input. These were used to isolate poor quality channels, reverse traces, monitor offsets and to give an overall assessment of noise levels. From these steps the exact nature of the field geometry was verified.

3) The near traces from every shot were displayed and inspected for poor or missing shots. These were additionally compared on a line-by-line basis to ensure acquisition consistency.

4) Single channel displays of any suspected or noisy traces to verify the nature and extent of any problems.

5) RMS noise analysis of noise files were conducted to determine background noise levels and verify any noisy channels.

6) RMS noise analysis within a window above the direct arrival for each shot and channel to determine noise levels along each sequence.

7) A brute stack was produced for each line. The processing sequence comprising geometry application, spherical divergence correction, NMO correction with a single regional velocity function, trace muting, stack and display.

2.2. Processing Sequence and Testing

The processing sequence was tested and devised by Peak Processing in June 2023.

The survey area was generally represented by a loose grid of 2D lines with a denser grid of lines covering three specific areas. The final sequence described hereafter, was derived and applied to all acquired lines, and checked for suitability across the survey area. The site shared similar geological characteristics and the chosen sequence was generally suitable throughout. Images in this report are taken from line OLE_OWF_M016.

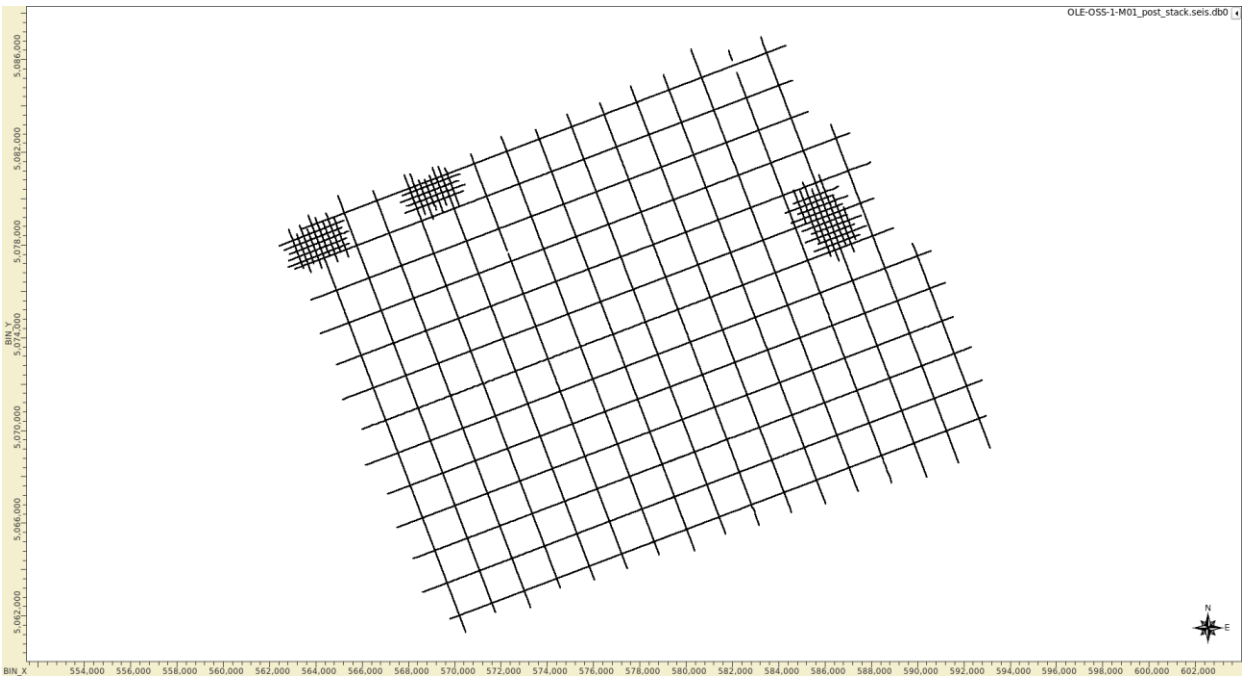

Figure 2 Full survey grid for all acquired lines

After re-formatting the data to an internal format, the near trace from all shots and selected shots in their entirety were displayed and analysed together with RMS noise analysis of shots used for quality control.

A recorder delay of -1ms was identified on the lines. An autocorrelation display was used to confirm the correct application.

After frequency analysis of the raw field data, it was deemed appropriate to resample the data to a lower sample rate due to little high frequency content. As such, the data was resampled from 0.0625ms to 0.125ms utilising an appropriate anti-alias filter. A low-cut bandpass filter of 160Hz was also applied to remove low frequency noise, well below the frequencies of interest.

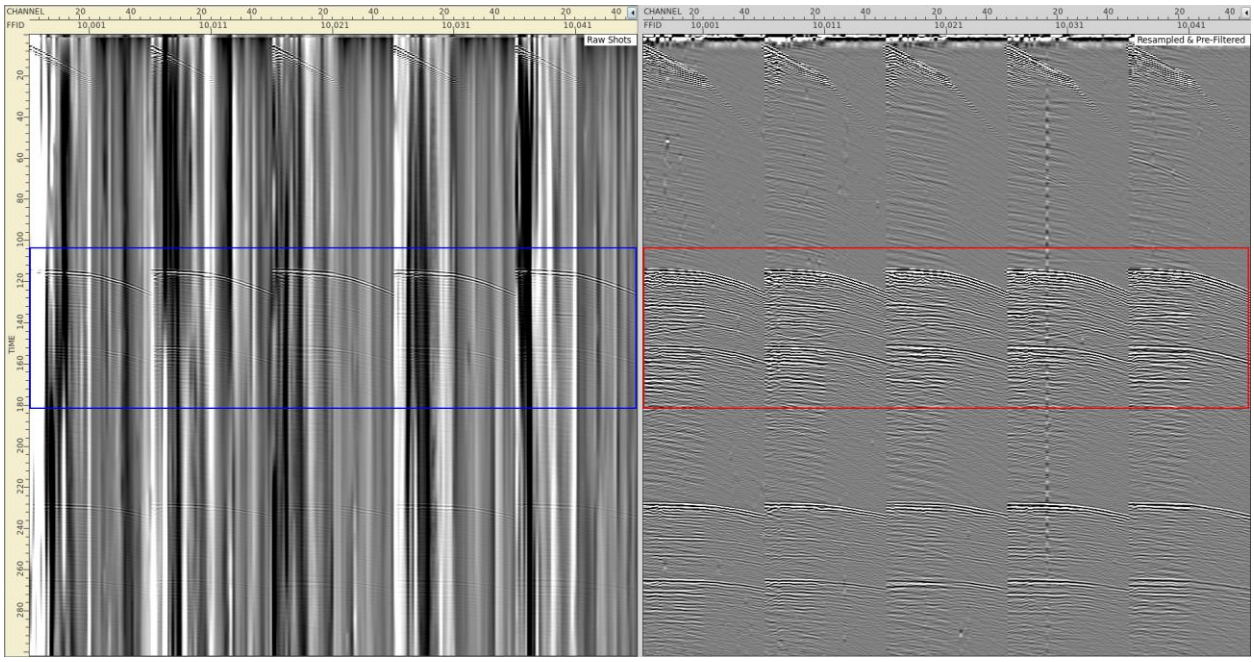

Figure 3 Shot record examples of raw shots before resampling (left/blue) and after pre-filter and resampling (right/red)

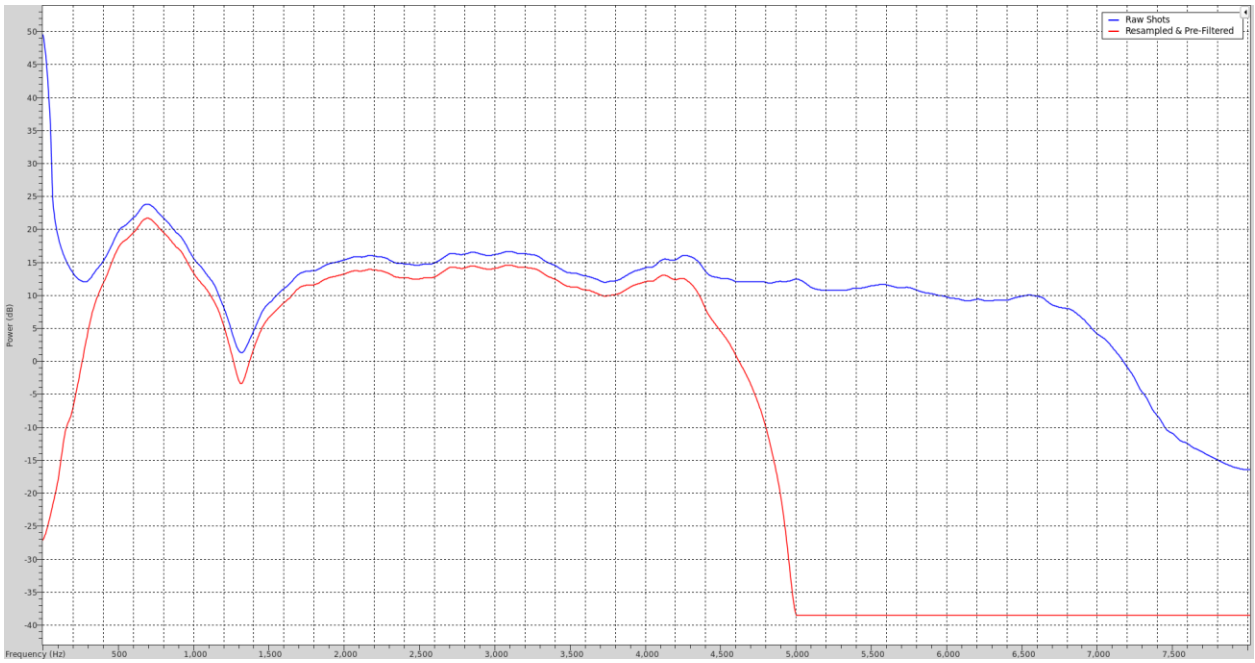

Figure 4 Frequency analysis of raw shots before resampling (left/blue) and after pre-filter and resampling (right/red)

Trace edits, including reverse channels, were identified and corrected and the exact nature of the field geometry was verified. Spiking channels were identified, killed and then infilled using a Fourier regularisation. Trace offset values were then assigned, and trace headers updated accordingly. The computed offsets were checked against the direct arrival times to ensure good compatibility.

A T^2 gain correction was applied, and a single function velocity field used to produce a brute stack.

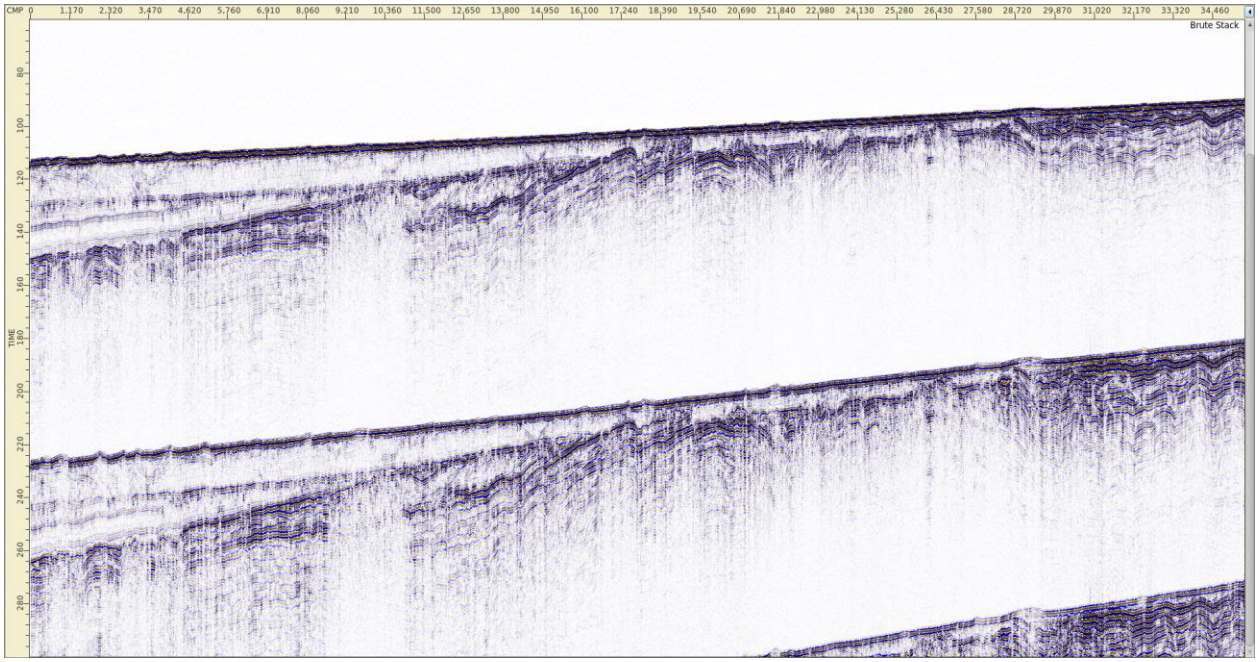

Figure 5 Brute Stack

Shots and QC stacks, after pre-filtering, displayed noise trends associated with sea surface swell noise and weather effects.

This effect typically causes a low frequency and discreet noise. The noise pattern is generally incoherent in a domain such as common offset, CMP or shot and can be easily removed. FX swell filters were applied to shots in several passes to remove noise trends related to swell and weather effects. FX swell filtering identifies noisy traces through noise threshold values and replaces them with a predicted value generated from FX prediction filters over a window of traces.

Best results were obtained using the parameters in the table below:

TRACE DOMAIN	TRACE WINDOW	TIME WINDOW (MS)	FREQUENCY BAND (HZ)	APPLICATION WINDOW (MS)	THRESHOLD
SHOT	3	60	0-2000	After 60	x8
SHOT	7	21	0-300	After 60	x3
SHOT	7	21	200-400	After 60	x3
SHOT	7	60	300-500	After 60	x4
SHOT	11	100	50-250	After 60	x4

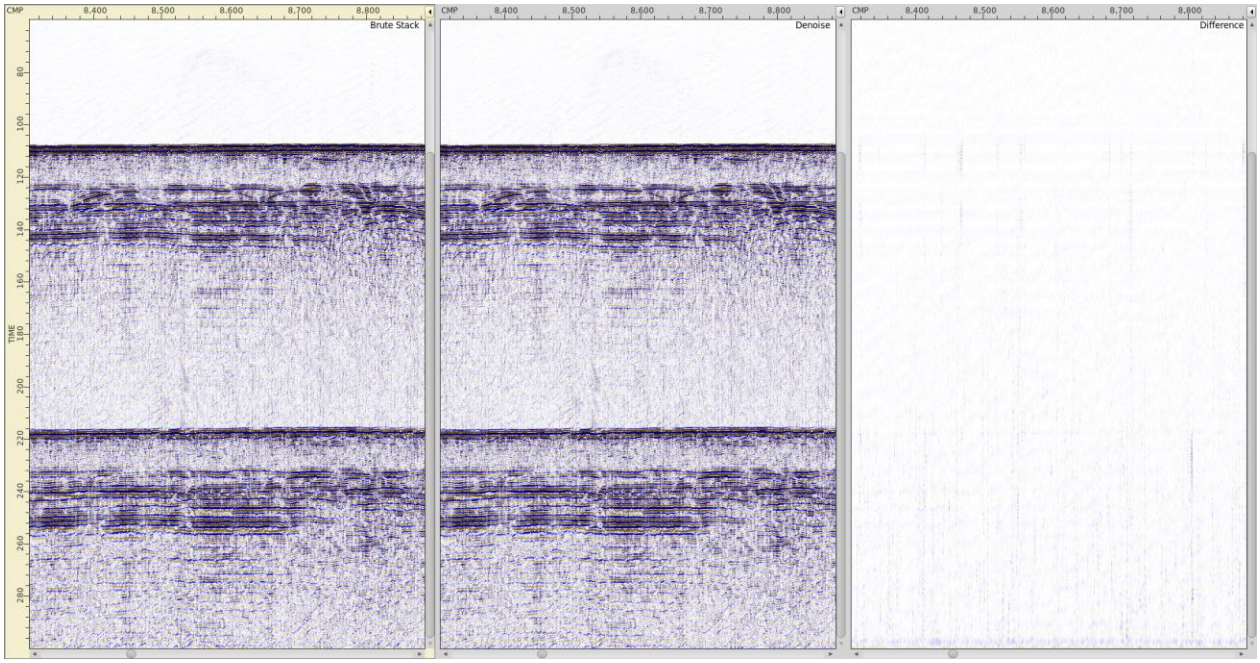

Figure 6 Stack example sub-section before denoise (left), after denoise (centre) and difference (right)

After removal of the swell and weather noise, the shots were interpolated such that they had a uniform receiver spacing of 1m. This was achieved by first applying a water velocity normal moveout function to the shots to loosely correct major reflectors for offset, before the application of a Fourier based interpolation to add traces such that the shot resembled a 72-trace streamer at a 1m receiver spacing. The water velocity moveout correction was then removed and the data sorted to CMP and stacked for QC purposes.

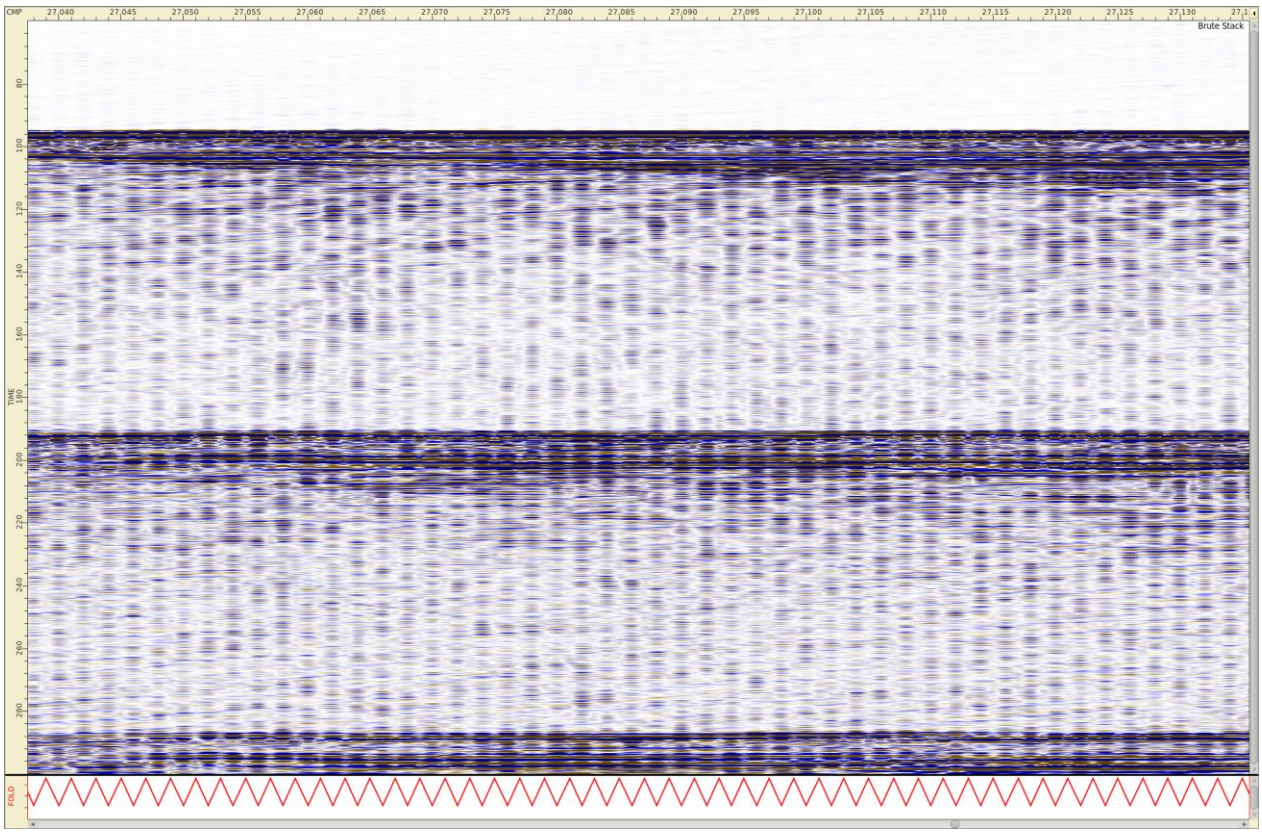

Figure 7 Sub-Section of Brute Stack, zoomed horizontally, showing trace fold header plot and irregular fold of cover

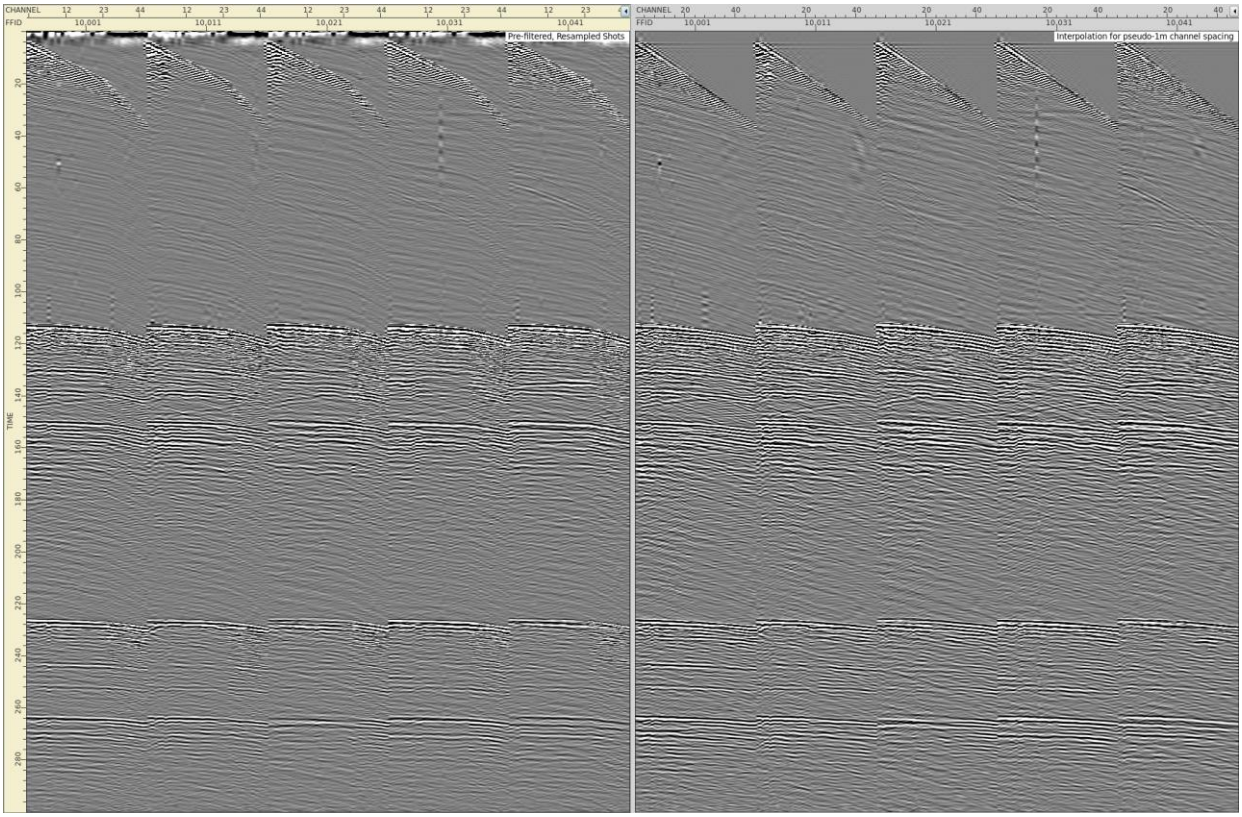

Figure 8 Selection of shots before interpolation (left) and after interpolation (right)

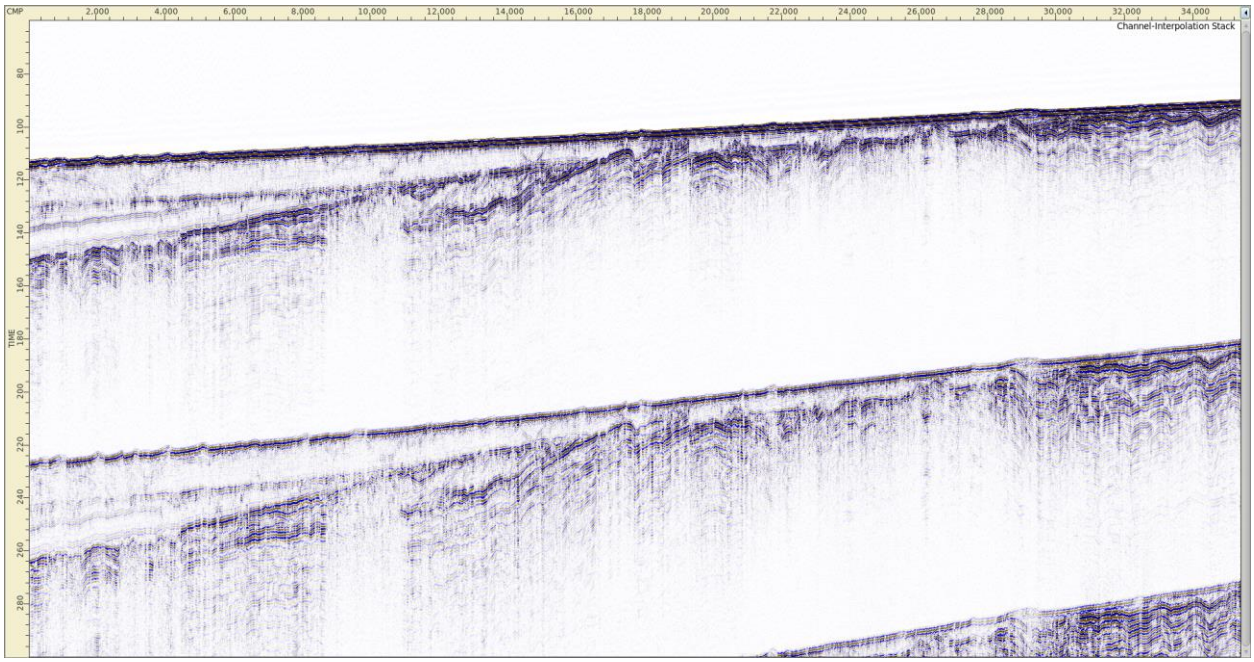

Figure 9 Stack example following interpolation to regularise channel spacing – nominal fold of is-36

Within ultra-high-resolution data, it is typical to have minor depth variations in the source and receiver tow depths. Given the vertical resolution, these variations are sufficient to cause a noticeable residual static within each shot and receiver position that impinges upon the coherency of CMPs and ultimately reduces the quality of the final stacks. To improve the coherency and interpretability of the data, a residual static solution was computed to correct for the depth variations. Given the variability of data quality, it was decided to use a pilot stack method for this purpose instead of a spatial common offset approach, as this type of approach typically requires a consistent data quality with this dataset displaying considerable variability due

to location and variable sea states throughout the survey. Correcting for the heave component provided a significant uplift to the coherency and corrected most of the residual static seen within the dataset.

A pilot stack was created for each line that provided a guide for calculating the residual values. A static correction value was then calculated for each trace that aligned to the pilot. These static values were written to the trace headers for application at a later stage in the processing. They were also applied to produce more coherent quality control stacks while monitoring individual processing steps.

Bathymetry for the site was loaded at this stage and, after conversion to time, it provided a quality control measure for the pilot stacks and for the static correction calculations.

The bathymetry was provided to the final datum and was therefore used to additionally calculate a pseudo-tidal value for each CMP for each line. This value was calculated by heavily smoothing the difference between the seismic seabed and the associated bathymetry, giving a slowly varying value approximating the shift required to correct the seismic data to the final datum. This pseudo-tidal static correction was also written to the trace headers for application after stacking.

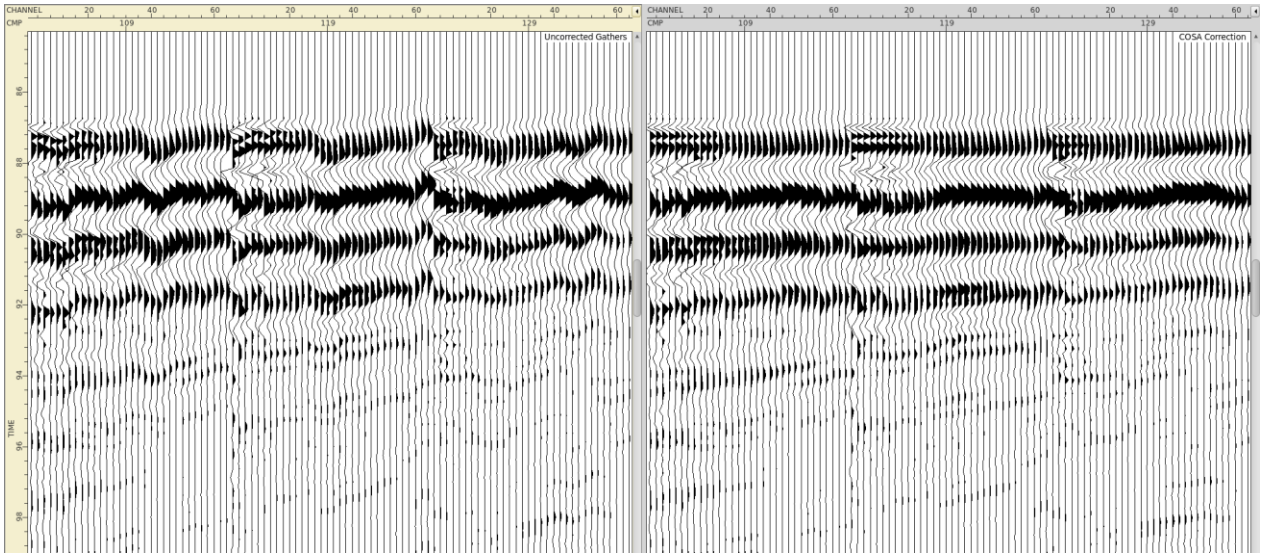

Figure 10 CMP examples (x3) before (left), and after (right), residual static correction with water velocity NMO applied

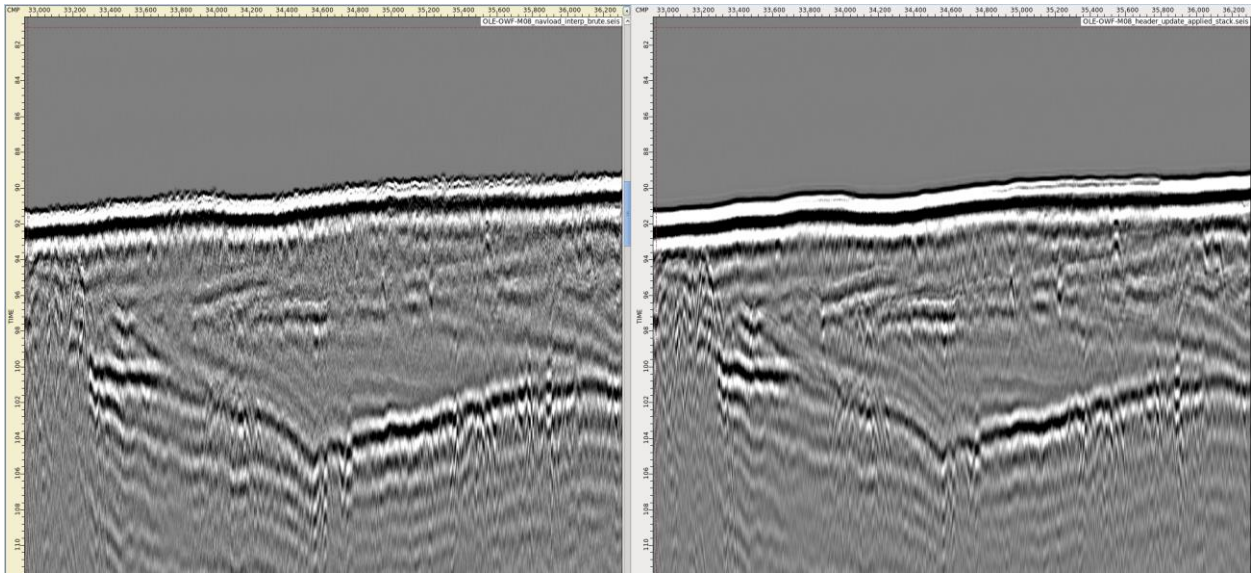

Figure 11 Stack subsection before (left), and after (right), residual static correction

At this stage of the processing, a further pass of FX Swell denoise was applied in the channel domain to further attenuate remnant random noise. A single pass of FX Swell denoise was applied, windowed to begin below 60ms TWT. A design window of 101 traces, and 12ms, was used to filter noise in a frequency range of 1000-2500Hz, above a threshold value of x12.

Coherent noise present was further addressed via a linear radon method. Firstly, a noise model based on an appropriate moveout value is produced, which was then adaptively subtracted from the input dataset.

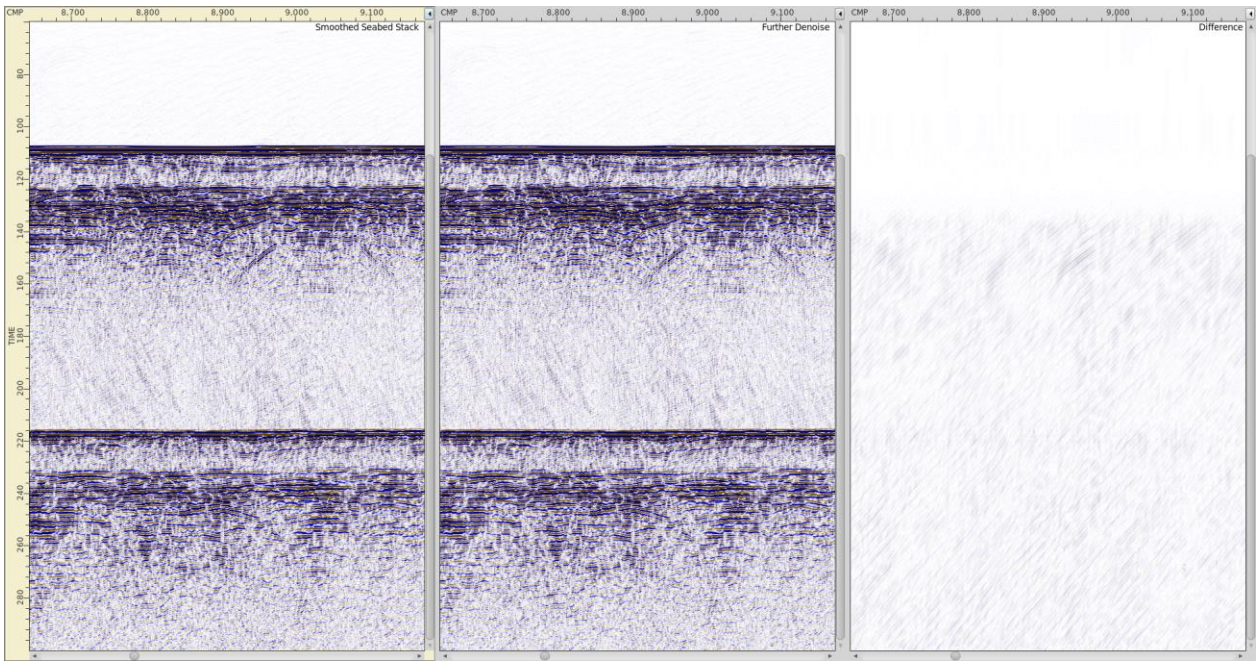

Figure 12 Stack subsection before (left), after (centre), and difference (right) with further denoise

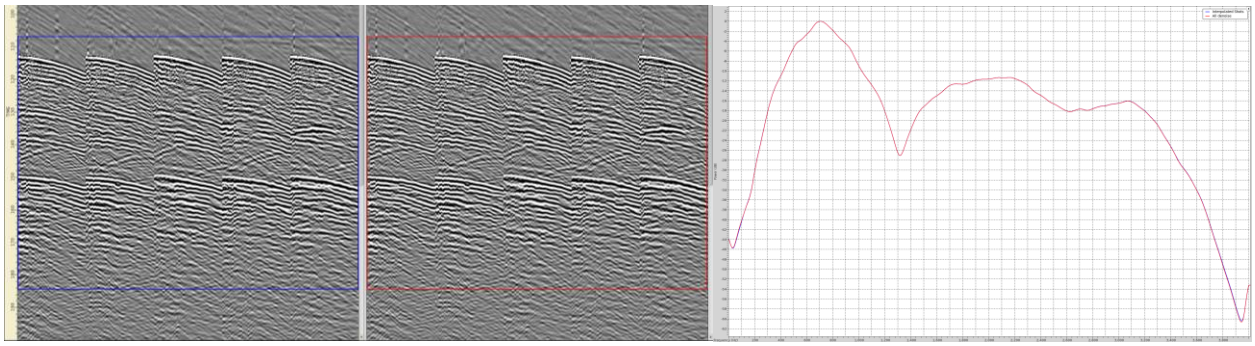

Figure 13 Example shot records and corresponding spectra before (left/blue) and after (right/red) further denoise (lines in spectral plot sit nearly on top of each other)

Sparker sources used in ultra-high-resolution surveys have a high energy output and a broadband high frequency content. However, they typically produce a long pulse with bubble oscillations and strong ghost artefacts. Following denoise processing and residual static computation, the source and receiver ghosts were attenuated, and the wavelet compressed and shaped to pseudo-zero phase. Achieving a good deghosting result relies on a good depth prediction for both the source and receivers.

Source deghosting was performed using an FK based deghosting algorithm parameterised with the target source depth as an initial input. Within a specified tolerance, the algorithm hunts for the best depth to apply for each shot before application.

Similarly, after source deghosting, receiver deghosting was applied using the target receiver depth as an initial input. Within a specified tolerance, the algorithm then further hunts for the best depth to apply for overlapping patches of receivers within shots.

Adaptive subtraction of the receiver ghost model helped to further attenuate the residual ghost related to the seabed reflection.

After deghosting, a zero-phasing operator was devised to shape the wavelet to pseudo-zero phase to assist with the interpretability of the data. This was achieved by extracting a field signature from a large range of shots over several survey lines before designing a shaping operator that is subsequently applied to the entire dataset.

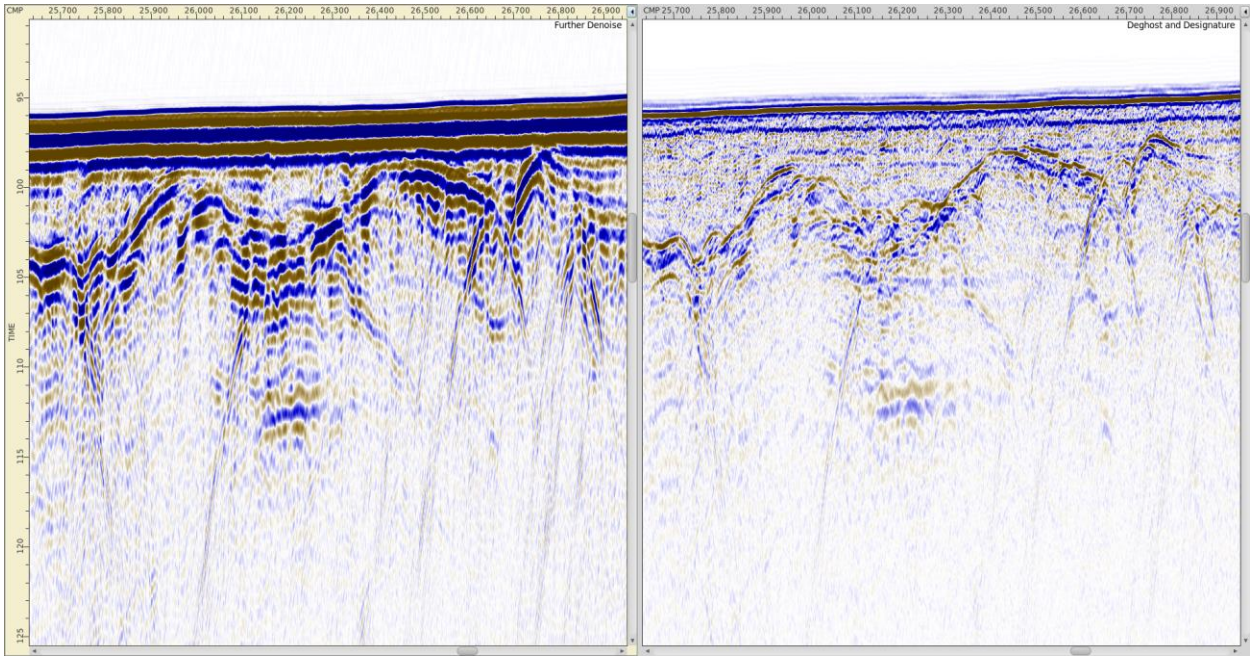

Figure 14 Stack subsection examples before (left) and after (right) denoise and designature

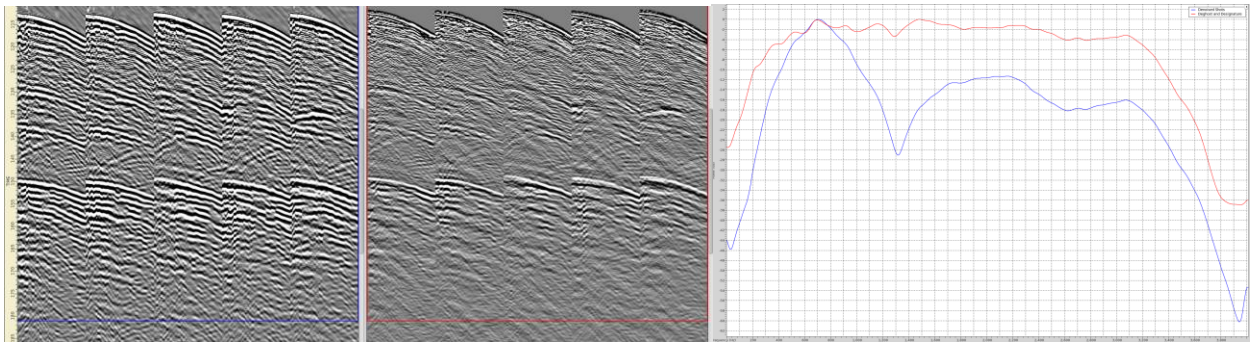

Figure 15 Example shot records and corresponding spectra before (left/blue) and after (right/red) deghost and designature

At this stage of the processing, 2D Surface Related Multiple Elimination (SRME) was tested and applied to remove surface related multiples in the data. SRME requires no user input to generate a multiple model as the input data is exclusively used for this purpose. Shots were prepared before generation of a multiple model for all shots and offsets. The multiple model was matched to the input data in shots and then adaptively subtracted from the input data in common channel order.

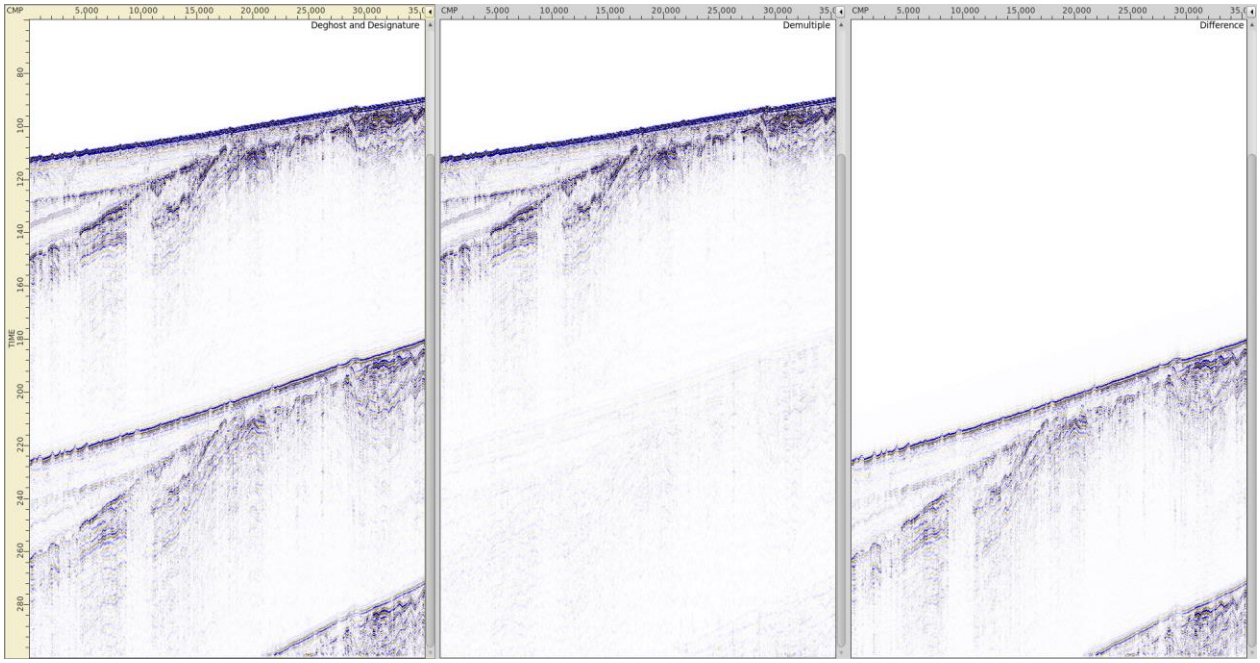

Figure 16 Subset stack examples before (left), after (centre) and difference (right) of SRME application

The residual static corrections computed at an earlier stage and described above, were applied at this stage before velocities were picked on semblance gathers at 500m intervals to define the velocity field for normal moveout correction and input into migration. The interactive velocity tools available in Reveal were used to pick and monitor consistency and quality.

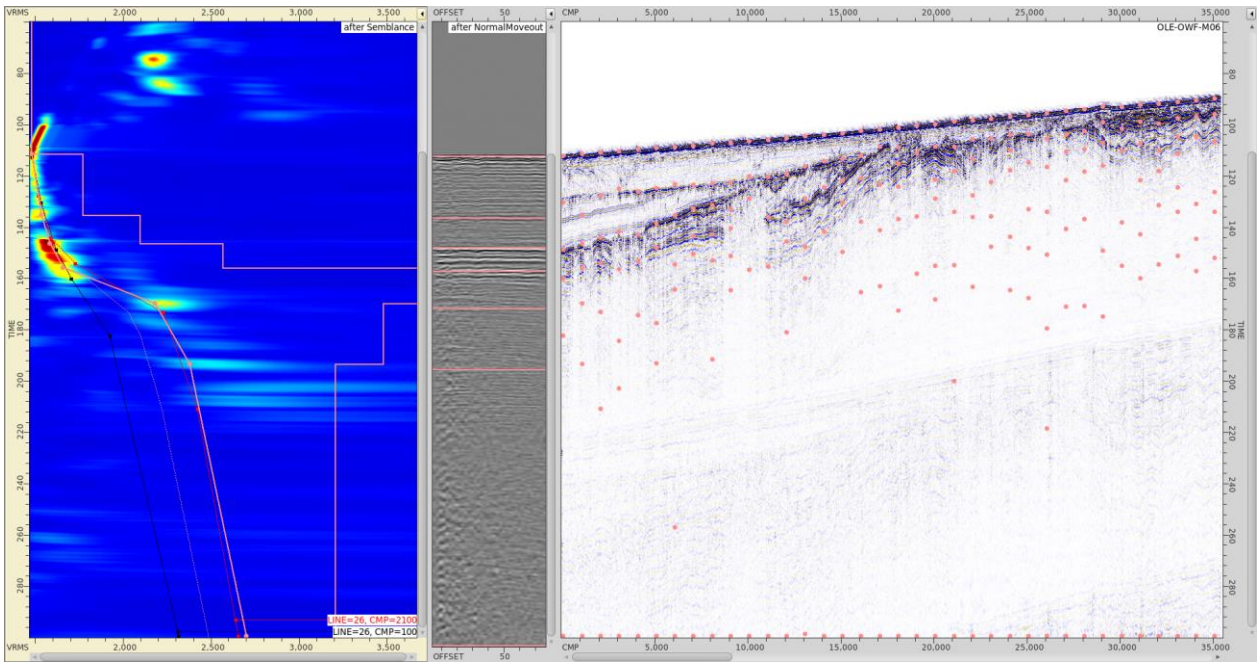

Figure 17 Velocity picking example with semblance display (left), representative gather (centre) and stack with velocity picks and overlay (right)

The velocity field was then prepared for input into 2D Pre-Stack Time Migration (PSTM). The T^2 gain function was removed prior to migration. The data was sorted to common offset before migration over the full frequency range using a 250m aperture. The 2D PSTM additionally corrects the gain for geometric spreading.

Figure 18 Stack example at PSTM stage

Figure 19 Stack subsection example at PSTM stage, zoomed over the shallow section

After migration, the data was sorted to common midpoint gathers and a final mute was selected and applied prior to stacking, utilising a 20 degree outside mute. The migrated, NMO corrected and muted data was then stacked using a mean function.

Post stack processing then followed to further improve the quality of the stacked data before final output.

Firstly, spectral shaping was applied to slightly enhance the higher frequency content within the stacked data.